

CONFIDENTIAL

Copy 1
RM SL54G15

NACA RM SL54G15

JUL 16 1954 RECD

CLASSIFICATION CANCELLED
AUTHORITY NASA TECHNICAL PUBLICATIONS
ANNOUNCEMENTS NO. _____ DATE _____ BY _____

Source of Acquisition
CASI Acquired



RESEARCH MEMORANDUM

CLASSIFICATION CHANGE

To: *Unclassified*
By authority of *NASA Memo Cite 52-23 /s/ by H-Maines*
Changed by *M. Ruda* Date *6-2-73*

for the

U. S. Air Force

LONGITUDINAL CONTROL CHARACTERISTICS OF A 1/20-SCALE MODEL
OF THE CONVAIR F-102 AIRPLANE AT TRANSONIC SPEEDS

By Robert S. Osborne and Kenneth E. Tempelmeyer

Langley Aeronautical Laboratory
Langley Field, Va.

Restriction/
Classification
Cancelled

This material contains information of the espionage laws, Title 18, U.S.C., in such a manner to an unauthorized person is prohibited by law.

of the United States within the meaning of the Espionage Laws, Title 18, U.S.C., the transmission or revelation of which in any

NATIONAL ADVISORY COMMITTEE FOR AERONAUTICS

WASHINGTON

JUL 14 1954

FILE COPY

To be returned to
the files of the National
Advisory Committee

for Aeronautics
Washington, D. C.

CONFIDENTIAL

14

CONFIDENTIAL

NATIONAL ADVISORY COMMITTEE FOR AERONAUTICS

RESEARCH MEMORANDUM

for the

U. S. Air Force

LONGITUDINAL CONTROL CHARACTERISTICS OF A 1/20-SCALE MODEL

OF THE CONVAIR F-102 AIRPLANE AT TRANSONIC SPEEDS

By Robert S. Osborne and Kenneth E. Tempelmeyer

SUMMARY

The effects of elevator deflections from 0° to -20° on the force and moment characteristics of a 1/20-scale model of the Convair F-102 airplane with chordwise fences have been determined at Mach numbers from 0.6 to 1.1 for angles of attack up to 20° in the Langley 8-foot transonic tunnel.

The configuration exhibited static longitudinal stability throughout the range tested, although a mild pitch-up tendency was indicated at Mach numbers from 0.85 to 0.95. Elevator pitch effectiveness decreased rapidly between the Mach numbers of 0.9 and 1.0; however, no complete loss or reversal was indicated for all conditions tested. Because of the type of longitudinal control used, trimming the configuration from the zero elevator condition resulted in substantial decreases in lift-curve slope and maximum lift-drag ratio and increases in drag due to lift. The drag at zero lift, drag due to lift, and trim drag were high for this configuration.

INTRODUCTION

At the request of the U. S. Air Force, a 1/20-scale model of the Convair F-102 airplane has been tested at transonic speeds in the Langley 8-foot transonic tunnel to determine its longitudinal stability and control characteristics.

In the initial phase of the investigation, the basic aerodynamic characteristics of the model with controls undeflected were determined and reported in reference 1. It was found that the basic configuration

CONFIDENTIAL

with a plain wing was subject to a severe pitch-up tendency at a lift coefficient of approximately 0.6 at high subsonic Mach numbers. Several wing fixes were tested in an attempt to alleviate the pitch-up tendency, with chordwise fences located at the 65-percent wing semispan station providing the most favorable results (see ref. 1).

The next phase of the investigation included determination of the effects of elevator deflections from 0° to -20° on the force and moment characteristics of the configuration with the chordwise fences at the 65-percent semispan station for Mach numbers from 0.6 to 1.1 and angles of attack up to 20° . The results are presented herein.

SYMBOLS

A	aspect ratio
A_E	duct exit area, sq ft
C_D	external drag coefficient, $C_{D_m} - C_{D_I}$
C_{D_I}	internal drag coefficient, D_I/qS
C_{D_m}	measured drag coefficient, D_m/qS
C_{D_0}	external drag at zero lift
$\frac{\partial C_D}{\partial C_L^2}$	drag-due-to-lift factor, averaged from $C_L = 0$ to $C_L = 0.3$
C_L	lift coefficient, L/qS
$C_{L(L/D)_{max}}$	lift coefficient for maximum lift-drag ratio
$\frac{\partial C_L}{\partial \alpha}$	lift-curve slope per degree, averaged from $\alpha = 0^\circ$ over linear portion of curve
$\frac{\partial C_L}{\partial \delta}$	lift effectiveness parameter at constant angle of attack
C_m	pitching-moment coefficient, $\frac{M_{cg}}{qS\bar{c}}$

$\frac{\partial C_m}{\partial C_L}$	static longitudinal stability parameter
$\frac{\partial C_m}{\partial \delta}$	pitch effectiveness parameter at constant lift coefficient
\bar{c}	wing mean aerodynamic chord, in.
D_I	internal drag, $m(V_O - V_E) - A_E(P_E - P_O)$, lb
D_m	measured drag, lb
L	lift, lb
$(L/D)_{\max}$	maximum lift-drag ratio
M	free-stream Mach number
M_{cg}	pitching moment about center-of-gravity location at 0.275 \bar{c} and 0.036 \bar{c} above wing-chord plane, in-lb
m	mass flow through inlets, slugs/sec
m_o	mass flow in free-stream tube of area equal to projected inlet area at $\alpha = 0^\circ$, slugs/sec
m/m_o	inlet mass-flow ratio
p_E	static pressure at duct exit, lb/sq ft
p_o	free-stream static pressure, lb/sq ft
q	free-stream dynamic pressure, lb/sq ft
S	wing area including fuselage, sq ft
V_E	velocity at duct exit, ft/sec
V_o	free-stream velocity, ft/sec
α	angle of attack of wing-chord line, deg
δ	elevator deflection with estimated correction for distortion, measured at right angles to hinge line and negative when trailing edge is up, deg

APPARATUS AND METHODS

Tunnel

The tests were conducted in the Langley 8-foot transonic tunnel, which is a dodecagonal, slotted-throat, single-return wind tunnel designed to obtain aerodynamic data through the speed of sound while minimizing the usual effects of blockage. The tunnel operates at approximately atmospheric stagnation pressures. Details of test-section design and flow uniformity are available in reference 2.

Model

The 1/20-scale model of the F-102 used in this investigation was supplied by the contractor and is shown in figure 1. Dimensional details are presented in figure 2.

The delta wing had 60° sweptback leading edges, 5° sweptforward trailing edges, and used NACA 0004-65 (mod.) streamwise airfoil sections with leading-edge radii of 0.18 percent chord. It was constructed with a steel leading edge and a tin-bismuth surface formed over a steel core. The chordwise fences were located at the 65-percent wing semispan station and extended from the leading edge to the elevators. The fence height from the 10- to 50-percent-chord stations was equal to the maximum local airfoil thickness.

The fuselage incorporated twin ram inlets (designed for the J-67 engine) with internal ducting to the jet exit at the model base. The base diameter was enlarged 0.3 inch (13.5 percent) over that for a true 1/20-scale model in order to insure that the duct flow would not be critical at the exit with the sting in place. Enlarging the base decreased the average boattail angle on the order of 1.5° . The vertical tail had the same plan form and airfoil sections as the wing semispan and included a flat-plate antenna located just above the rudder.

The configuration had no horizontal tail. The elevators were wing trailing-edge flaps deflected about hinge lines perpendicular to the model center line. The total elevator area rearward of the hinge line was 10.2 percent of the total wing area. The wing elevator gap ahead of the hinge line was sealed.

Additional model details such as airfoil ordinates and a cross-sectional area distribution are available in reference 1.

Model Support System

The model was attached to a strain-gage balance located inside the fuselage. The sting support was cylindrical for a distance of 3.2 base diameters rearward of the model base, and at its downstream end was attached to a support tube through couplings which were varied to keep the model near the center of the tunnel at all angles of attack. The support tube was fixed axially in the center of the tunnel by two sets of support struts projecting from the tunnel walls.

Measurements and Accuracy

The test Mach number was determined to within ± 0.003 from a calibration with respect to the pressure in the chamber surrounding the slotted test section.

Lift, drag, and pitching moment were determined from an internal strain-gage balance. The pitching moment was measured about a center-of-gravity location at 27.5 percent of the mean aerodynamic chord and 3.6 percent of the mean aerodynamic chord above the chord plane. The force and moment coefficients were estimated to be accurate within the following limits up to a lift coefficient of at least 0.4: C_L , ± 0.005 ; C_{D_m} , ± 0.001 ; C_M , ± 0.001 .

The mass flow through the ducts and the internal drag were determined from separate tests using pressure measurements made with a survey rake located at the model base. The internal drag coefficients were estimated to be accurate within ± 0.001 .

The angle of attack was determined to within 0.15° from a fixed-pendulum strain-gage unit located in the support sting and from a calibration of sting and balance deflection with respect to model load. The 0° elevator setting was locked in position and was estimated to be accurate within 0.1° . The other elevator settings, requiring corrections for distortion due to load, were probably accurate to within 0.5° .

Tests

The model was tested at Mach numbers from 0.6 to 1.1 at angles of attack from 0° to approximately 20° with elevator deflections of 0° , -5° , -10° , -15° , and -20° . At the higher Mach numbers, the maximum attainable angle of attack was reduced to less than 20° by tunnel power and balance limitations.

All tests were run with air flow through the ducts; however, internal flow characteristics were measured only for the 0° elevator case at angles of attack up to 15° .

The test Reynolds number based on the wing mean aerodynamic chord was of the order of 4.5×10^6 (fig. 3).

Corrections

The slotted walls of the test section minimize subsonic boundary interference effects, and no corrections for this interference have been applied.

The effects of supersonic boundary-reflected disturbances were reduced by testing the model a few inches off the tunnel center line. However, these disturbances probably caused the measured drag at low lift coefficients to be slightly high at Mach numbers near 1.05 and slightly low at a Mach number of approximately 1.10. These errors have been minimized by judicious fairing of all drag data except for the measured drag in figure 5, and it is believed that none of the general trends exhibited by these faired data or the conclusions drawn therefrom were affected by boundary-reflected disturbances.

No corrections for sting interference have been applied. Sting effects should be small, however, since the flow through the internal ducting system surrounds the sting as it leaves the jet exit.

The 0° elevator was locked in position and no correction for distortion of the elevator due to air load was applied. The other elevator settings were not restrained as rigidly, however, and corrections for distortion due to load have been applied. These corrections were determined by comparison of the present data with unpublished data obtained from tests of a similar configuration employing relatively rigid elevators in the Langley 8-foot transonic tunnel.

It was estimated that the approximately 1.5° decrease in boattail angle for the model tested as compared with that for a true 1/20-scale model resulted in a decrease in external drag coefficient which was well within the accuracy of the data, and no correction has been applied.

RESULTS

All tests were run with the ducts open; however, inlet mass-flow ratios and internal drag coefficients were obtained for the zero-elevator-deflection case only and are presented in figure 4.

The basic force and moment characteristics of the model with various elevator deflections are presented as a function of lift coefficient at constant Mach number in figure 5. The measured drag data presented in this figure include both the internal and external drag.

The lift coefficients required for level flight of the F-102 airplane at a combat wing loading of 35.4 lb/sq ft have been calculated for altitudes from sea level to 60,000 feet and are presented in figure 6.

Summary and analysis data are presented in figures 7 to 14. Drag data used in figures 10 to 14 have had the internal drag of figure 4 removed. In subtracting the internal drag for the zero-elevator-deflection case from data with elevator angles from 0° to -20°, the reasonable assumption has been made that elevator deflection had no effect on the model's internal flow characteristics.

DISCUSSION

Pitching-Moment Characteristics

Static longitudinal stability.- The configuration exhibited static longitudinal stability for all elevator angles and lift coefficients tested (fig. 5); however, there were nonlinearities in the pitch curves for some elevator deflections in the trim region at Mach numbers from 0.85 to 0.95. The results of dynamic response calculations (ref. 3, for example) indicate that these nonlinearities could cause mild pitch-up. It was apparent, however, that over the elevator-deflection range tested the chordwise fences installed on the wings had been successful in substantially reducing the severe pitch-up associated with the plain wing (see ref. 1).

Values of the static longitudinal stability parameter $\frac{\partial C_m}{\partial C_L}$ taken at lift coefficients for trimmed level flight for altitudes from sea level to 60,000 feet (see fig. 6) varied from -0.075 at a Mach number of 0.6 to approximately -0.185 at Mach numbers above 1.0 (fig. 7), an indication of a rearward shift in aerodynamic-center location of approximately 11 percent of the mean aerodynamic chord. The effects of increasing the altitude on the parameter were small, although the variation of $\frac{\partial C_m}{\partial C_L}$ with Mach number for an altitude of 60,000 feet was more irregular than for the lower altitudes. Although these data indicated that, in general, no serious static longitudinal stability problem existed for the airplane in the speed and lift range tested, it should be noted that

the forward shift in aerodynamic-center location which would occur with a rapid decrease in speed on entering a turn at a Mach number of 1.0, for example, could aggravate an otherwise mild pitch-up tendency.

Elevator pitch effectiveness.- The elevator pitch effectiveness parameter $\frac{\partial C_m}{\partial \delta}$ at constant lift coefficient was essentially constant for an elevator-deflection range from 0° to -10° and for lift coefficients from 0 to 0.4. The average value of $\frac{\partial C_m}{\partial \delta}$ for this elevator-deflection and lift-coefficient range reached a maximum value of -0.0061 at a Mach number of 0.9 and then decreased in magnitude about 35 percent with an increase in Mach number to 1.0 (fig. 7).

It should be noted that while any parameter herein involving an absolute value of elevator deflection must be viewed with caution because of possible inaccuracies in estimating the effects of elevator distortion due to aerodynamic load, it is felt that such phenomena as the loss of elevator effectiveness shown in figure 7 were, because of their abruptness and magnitude, real and were not the result of deflections due to load.

Increasing the lift coefficient above 0.4 at Mach numbers from 0.9 to 1.0 or increasing elevator deflection above 10° at subsonic Mach numbers resulted in lower pitch effectiveness than that shown in figure 7; however, no complete loss or reversal was indicated anywhere in the range tested (see fig. 5).

Trim elevator settings.- Elevator deflections required for trimmed level flight at several altitudes for a wing loading of 35.4 lb/sq ft are indicated in figure 8. Large increases in up elevator, an indication of control-position instability, were evident in the Mach number range from 0.925 to 1.0. The increase in control deflection required increased with altitude, as would be expected. The control-position instability was the result of a combination of decreased elevator pitch effectiveness and increased out-of-trim pitching moment with the controls undeflected (see figs. 5 and 7).

Lift Characteristics

Lift-curve slopes.- The lift curves for the various elevator angles at constant Mach number were generally linear for angles of attack up to 12° or 16° (fig. 5). Gradual decreases in lift-curve slope occurred as the angle of attack was increased to 20° .

The lift-curve slope averaged over the linear portion of the curve varied from 0.044 to 0.052 for the 0° elevator case (fig. 9). With increases in elevator deflection, minor increases in average lift-curve slope were indicated at Mach numbers above 0.8 (fig. 5).

Effects of trim.- Trimming the configuration reduced the untrimmed ($\delta = 0^\circ$) lift-curve slope by 20 to 30 percent. This substantial loss is a result of the type of longitudinal control used. In order to provide trim, the elevators, which are trailing-edge flaps comprising 10 percent of the total wing area, must be deflected trailing edge up, thus decreasing the lift at a given angle of attack. Since the elevators have a relatively short effective tail length and therefore require large areas and deflections in order to produce the necessary longitudinal balancing moments, these losses in lift are large.

Elevator lift effectiveness.- The lift effectiveness of the elevators as indicated by the rate of change of lift coefficient with elevator deflection at constant angle of attack $\frac{\partial C_L}{\partial \delta}$ decreased from 0.020 at sub-critical speeds to 0.013 at Mach numbers above 1.0 (fig. 9). These values are applicable to and have been averaged over an angle-of-attack range from 0° to 8° for elevator deflections from 0° to -10° . As indicated in figure 5, the lift effectiveness decreased only slightly at higher angles of attack; however, it approached zero for elevator deflections above 15° at Mach numbers above 0.95.

Drag Characteristics

Zero-lift drag.- The abrupt rise in zero-lift drag for the configuration with elevators undeflected began at a Mach number of approximately 0.91 (fig. 10). The magnitude of the drag rise was approximately 0.019 between the Mach numbers of 0.85 and 1.05 and was rather large because of the unfavorable axial distribution of total cross-sectional area of the model. A more complete discussion of this is included in reference 1.

Substantial increases in zero-lift drag at constant Mach number were indicated with increases in elevator deflection above -5° (see fig. 5).

Drag due to lift.- For the zero-elevator-deflection case, the value of drag-due-to-lift factor $\frac{\partial C_D}{\partial C_L^2}$, averaged over a lift-coefficient range from 0 to 0.3, remained essentially constant at 0.26 over the Mach number range tested (fig. 10). The drag-due-to-lift factor for the F-102 wing, assuming full leading-edge suction (approximately equal to $1/\pi A$ for Mach numbers below 1.05), was about 0.145. (See ref. 1.) The drag due to

lift for no leading-edge suction (equal to $\frac{1}{57.3 \frac{\partial C_L}{\partial \alpha}}$) was of the order

of 0.35. It indicated, therefore, that only about 45 percent full leading-edge suction was being realized. In general, the drag due to lift increased with increasing elevator deflection (fig. 5).

A comparison of lift-drag polars for the zero-elevator-deflection case with those for trimmed conditions (fig. 11) indicated the severe drag penalty paid for trimming the configuration. The increase in drag due to lift caused by trimming varied from approximately 45 percent at a Mach number of 0.6 to 120 percent at a Mach number of 1.1 (fig. 10). As has been indicated previously, the large penalty for trimming was the result of the wing-trailing-edge-flap type of longitudinal control used. The increase in trim effects at Mach numbers above 0.9 was due to the increased pitching-moment increment required to trim combined with decreased control effectiveness.

Lift-drag ratios.- The maximum lift-drag ratios for the configuration with the elevators undeflected decreased from approximately 10.5 at subcritical speeds to 5.8 at Mach numbers above 1.0 (fig. 12). The lift coefficient for maximum lift-drag ratio increased from 0.17 at a Mach number of 0.6 to 0.29 at Mach numbers above 1.0 (fig. 12). Trimming the configuration reduced the maximum lift-drag ratio by about 2.0 over the Mach number range tested and decreased the lift coefficient for maximum lift-drag ratio by approximately 0.05 (fig. 12). As previously discussed, this was due to large increases in drag due to lift for trim conditions.

The lift-drag ratios for trimmed level flight at various altitudes are compared with the maximum possible trimmed lift-drag ratios in figure 13. It is of interest to note the increase in altitude for most efficient flight with increasing Mach number. It was indicated that flight at maximum trimmed lift-drag ratio would occur at an altitude of 20,000 feet at a Mach number of 0.6, 40,000 feet at Mach numbers from 0.85 to 0.95, and 60,000 feet at a Mach number of 1.1. The advantages of cruising at high altitude were apparent from these data.

Contributing drag factors.- The drag values for trimmed level flight of the configuration at altitudes from sea level to 60,000 feet have been broken down into several component parts in order to show their relative importance for various flight conditions (fig. 14). The first component, skin-friction drag, has been taken as the subsonic drag level at zero lift. The minimum wave drag is the difference between the skin-friction and total drag at zero lift and is the component which depends upon the axial distribution of cross-sectional area of the model (see ref. 3). The drag-due-to-lift component is the difference between the zero-lift drag and the drag at the lift coefficient required with the elevators undeflected. This component is a function of wing characteristics such

as aspect ratio, leading-edge sweep, and leading-edge radius. The last component, trim drag, is the additional drag increment caused by trimming the configuration from the zero elevator condition. It depends on the type of control, magnitude of the out-of-trim pitching moments, and the control effectiveness.

At altitudes of sea level and 20,000 feet, the drag at subcritical Mach numbers was mostly skin friction, whereas at transonic speeds the wave drag became the most important component. At an altitude of 40,000 feet, the drag due to lift and trim drag comprised the larger part of the total drag at subcritical speeds, the wave drag continuing to be the predominant factor at higher Mach numbers. At an altitude of 60,000 feet, the drag due to lift and trim drag were the largest components through the Mach number range, although the wave drag was still an important factor at transonic speeds. It is apparent that in order to improve the medium and high-altitude performance of the configuration all three of the major drag components - wave drag, drag due to lift, and trim drag - should be appreciably reduced.

CONCLUSIONS

The following conclusions may be drawn from a wind-tunnel investigation of the longitudinal stability and control characteristics of a 1/20-scale model of the Convair F-102 airplane at transonic speeds:

1. The configuration exhibited static longitudinal stability for all conditions tested; however, the possibility of mild pitch-up was indicated at Mach numbers from 0.85 to 0.95.
2. Elevator lift and pitch effectiveness decreased rapidly between the Mach numbers of 0.9 and 1.0, but no complete loss or reversal of pitch effectiveness was indicated in the range tested.
3. The trailing-edge-flap type of longitudinal control resulted in substantial decreases in lift-curve slope and maximum lift-drag ratio and increases in drag due to lift when the configuration was trimmed from the zero elevator condition.

4. The configuration had high transonic drag at zero lift, high drag due to lift with the elevators undeflected, and high drag due to trim.

Langley Aeronautical Laboratory,
National Advisory Committee for Aeronautics,
Langley Field, Va., June 29, 1954.

Robert S. Osborne

Robert S. Osborne
Aeronautical Research Scientist

Kenneth E. Tempelmeyer

Kenneth E. Tempelmeyer
Aeronautical Research Scientist

Approved:

Eugene C. Draley

Eugene C. Draley
Chief of Full-Scale Research Division

MML

REFERENCES

1. Osborne, Robert S., and Wornom, Dewey E.: Aerodynamic Characteristics Including Effects of Wing Fixes of a 1/20-Scale Model of the Convair F-102 Airplane at Transonic Speeds. NACA RM SL54C23, U. S. Air Force, 1954.
2. Ritchie, Virgil S., and Pearson, Albin O.: Calibration of the Slotted Test Section of the Langley 8-Foot Transonic Tunnel and Preliminary Experimental Investigation of Boundary-Reflected Disturbances. NACA RM L51K14, 1952.
3. Roderick, H.: Investigation of Pitch Up Effects on the F-102 Airplane. Dynamics Memo DC-8-134 (Contract #AF33(600)-5942), Consolidated Vultee Aircraft Corp., July 30, 1953.
4. Whitcomb, Richard T.: A Study of the Zero-Lift Drag-Rise Characteristics of Wing-Body Combinations Near the Speed of Sound. NACA RM L52H08, 1952.

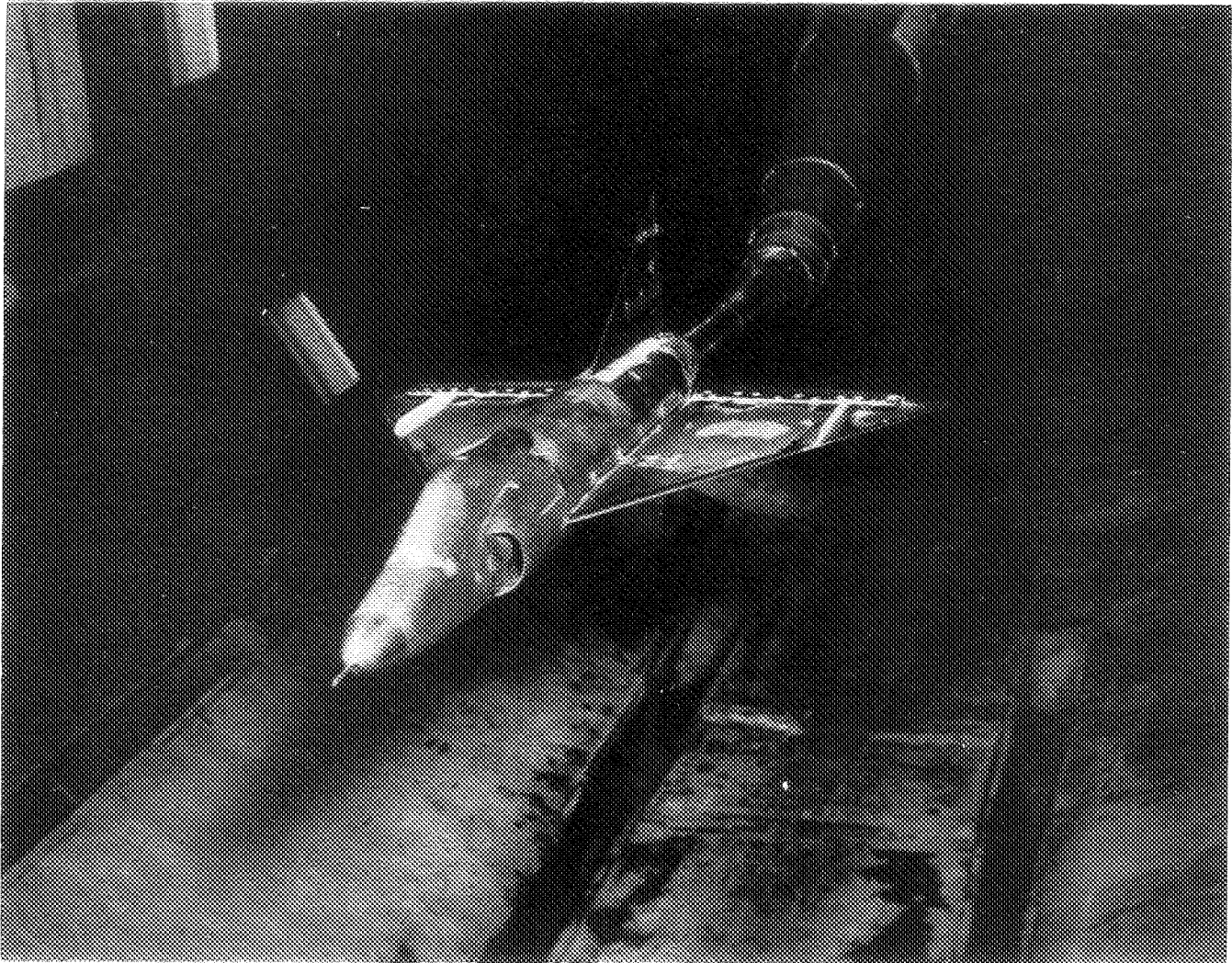
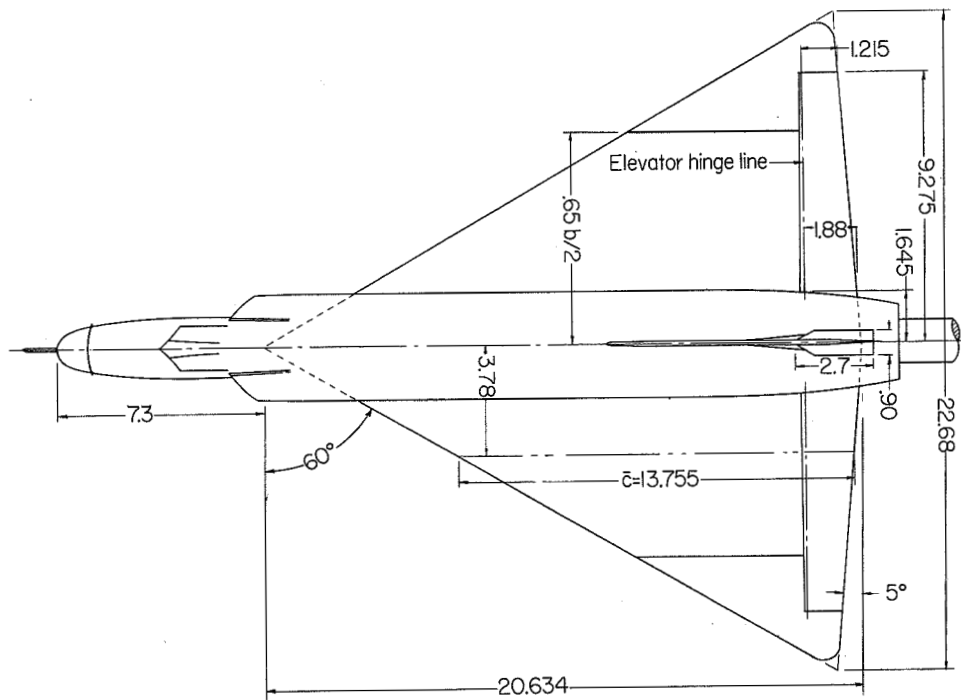
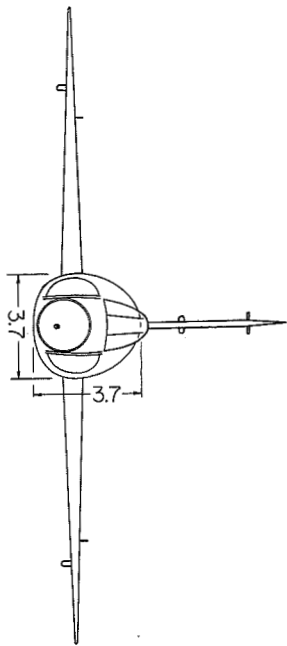


Figure 1.- Photograph of the 1/20-scale model of the Convair F-102 airplane as tested in the Langley 8-foot transonic tunnel.

L-76591



Wing details

Airfoil section	NACA 0004-65 (Modified)
Area, sq ft	1.625
Aspect ratio	2.2
Incidence, deg	0
Dihedral, deg	0
Elevator area aft of hinge line, sq ft	0.166

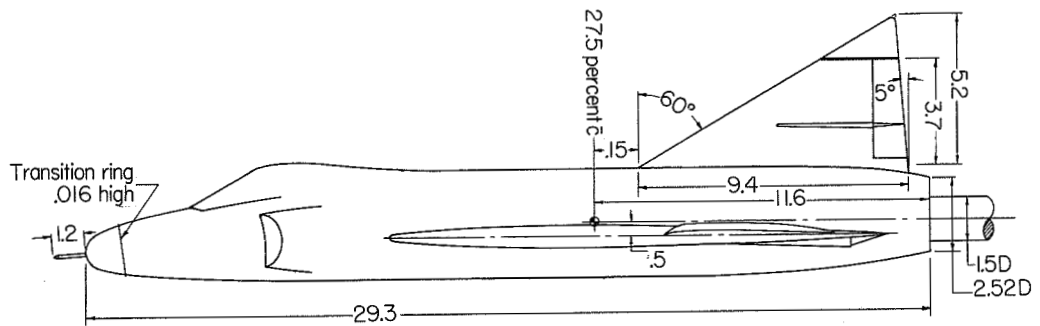


Figure 2.- Model details. All dimensions are in inches unless otherwise noted.

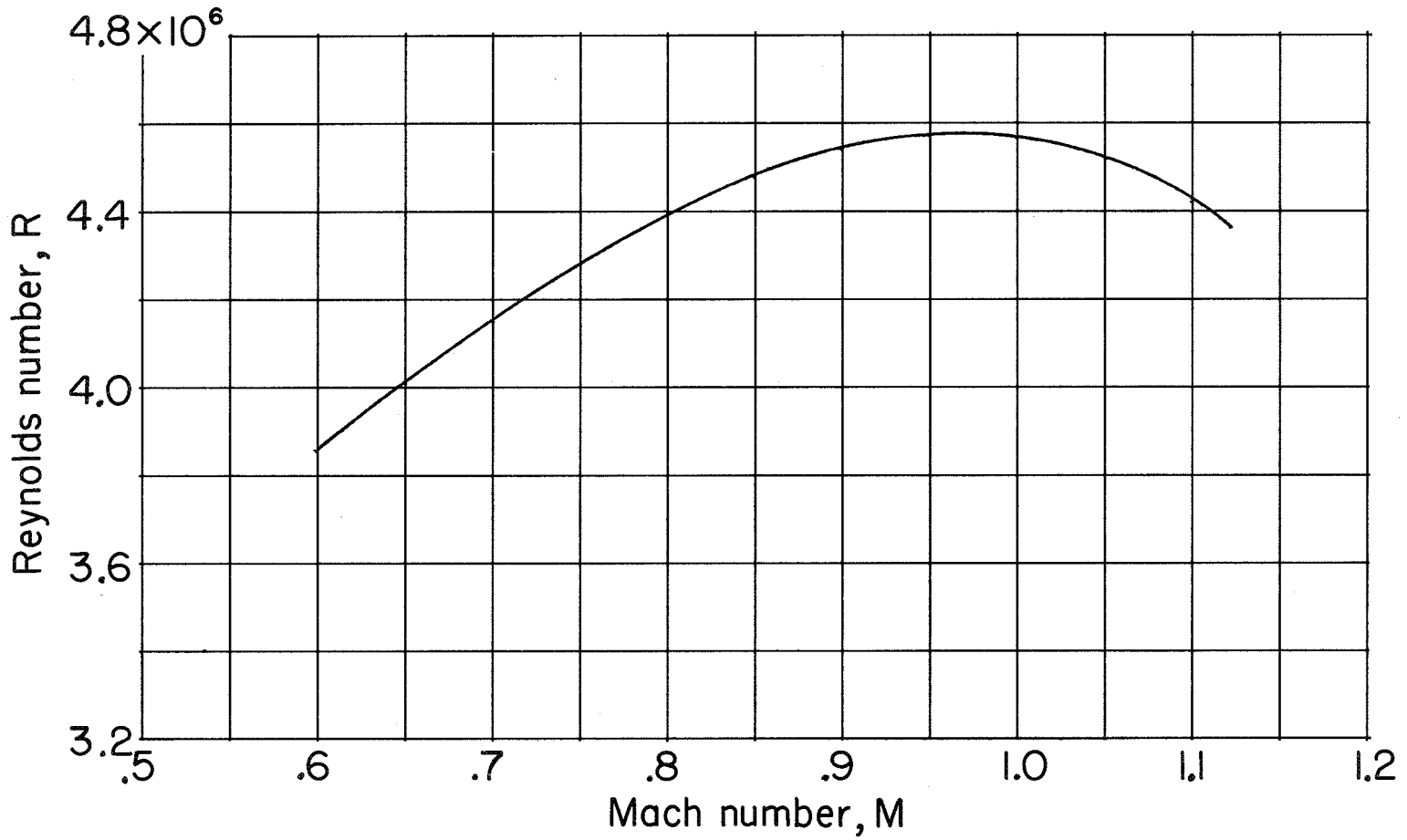


Figure 3.- Variation with Mach number of the approximate test Reynolds number based on $\bar{c} = 13.755$ inches.

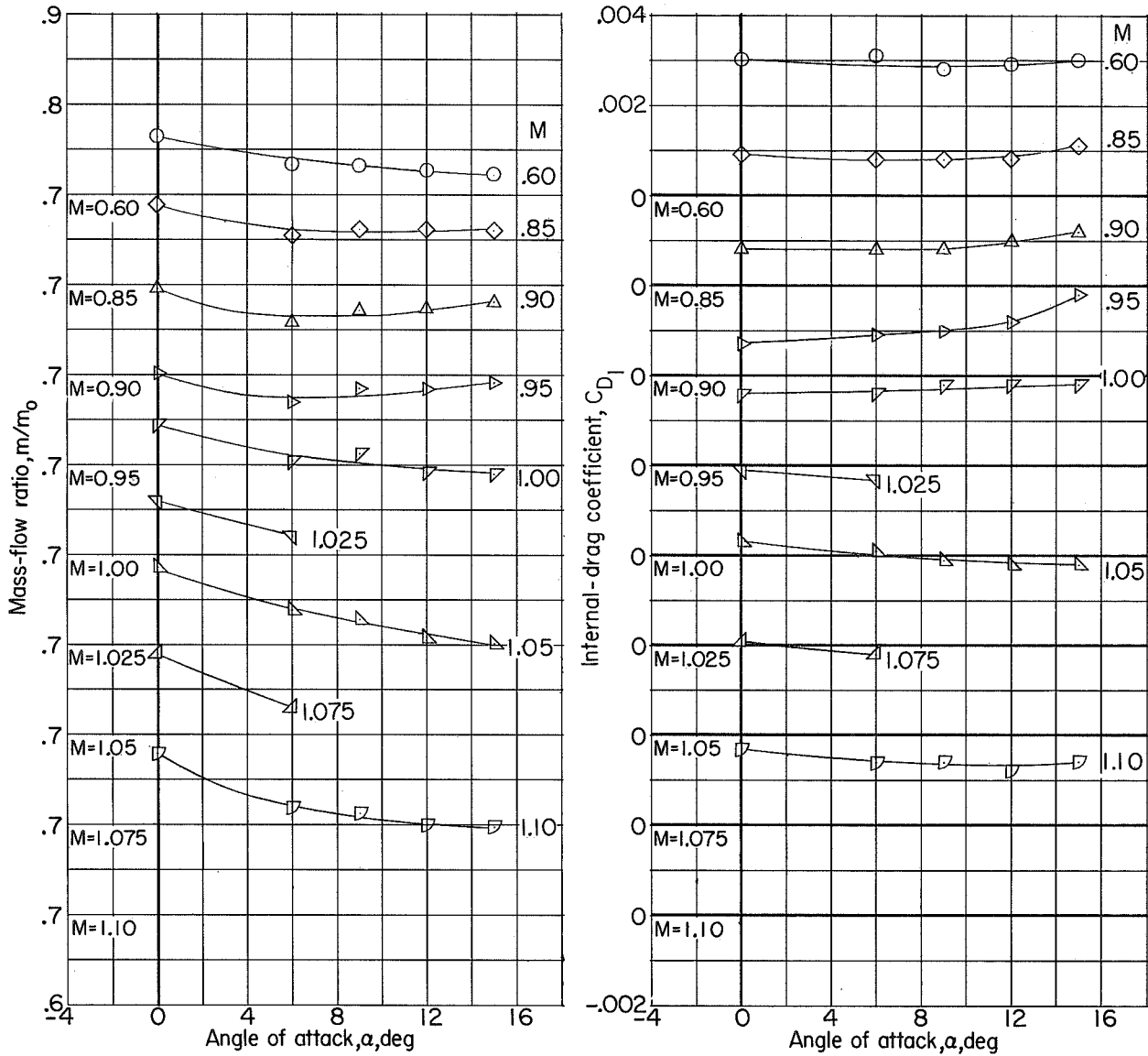
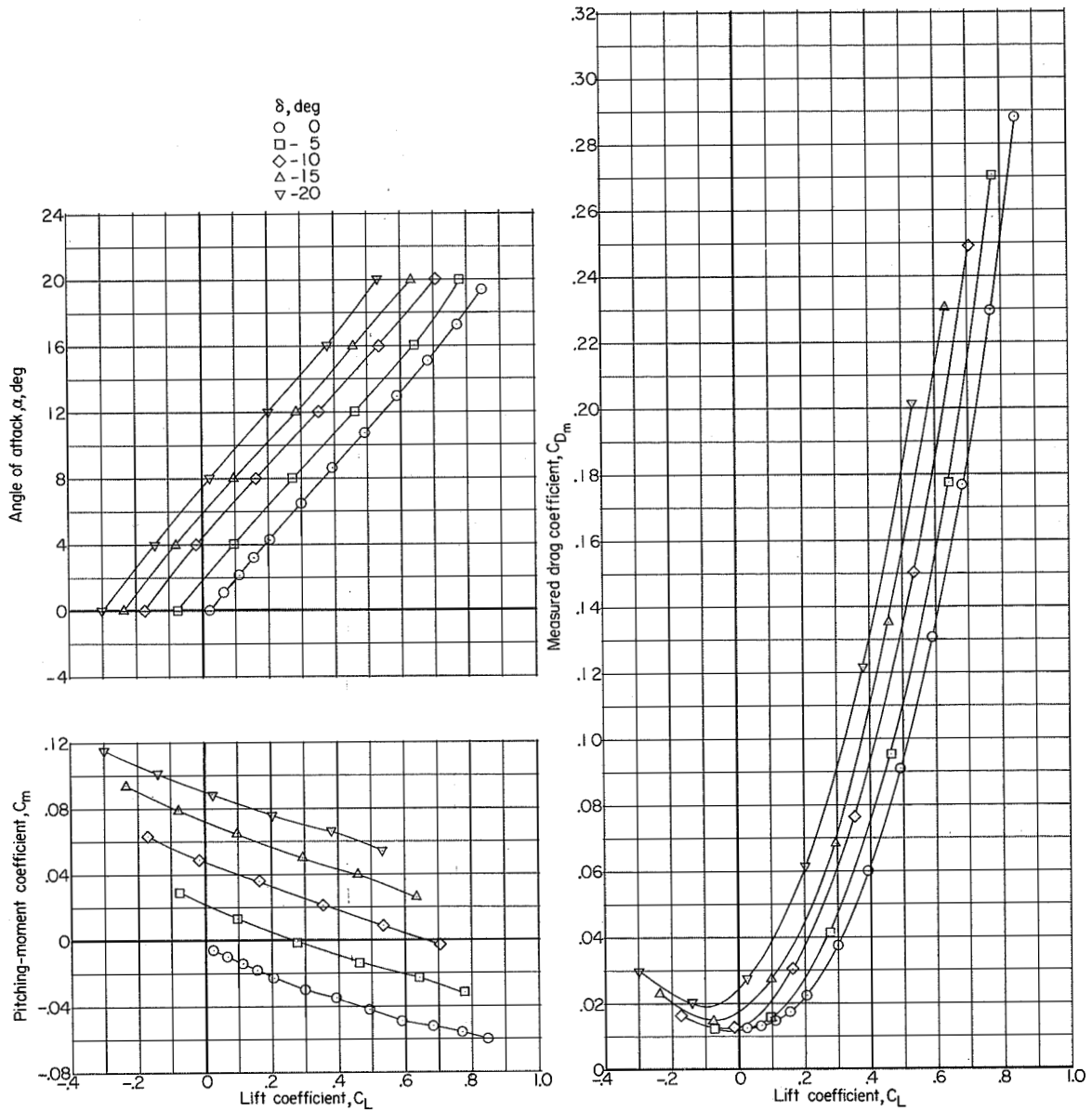
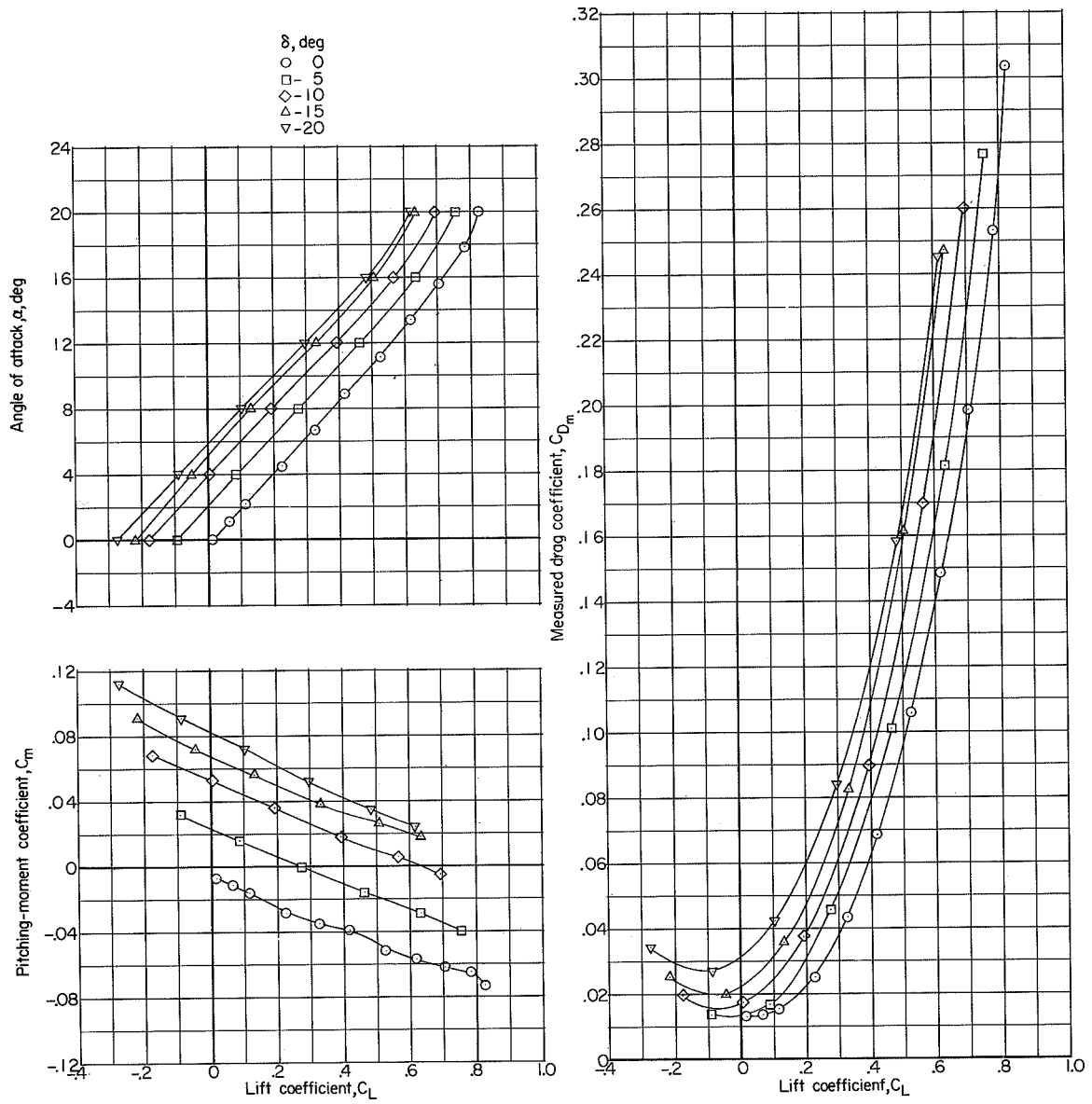


Figure 4.- Mass-flow ratios and internal drag coefficients for the model with 0° elevator deflection.



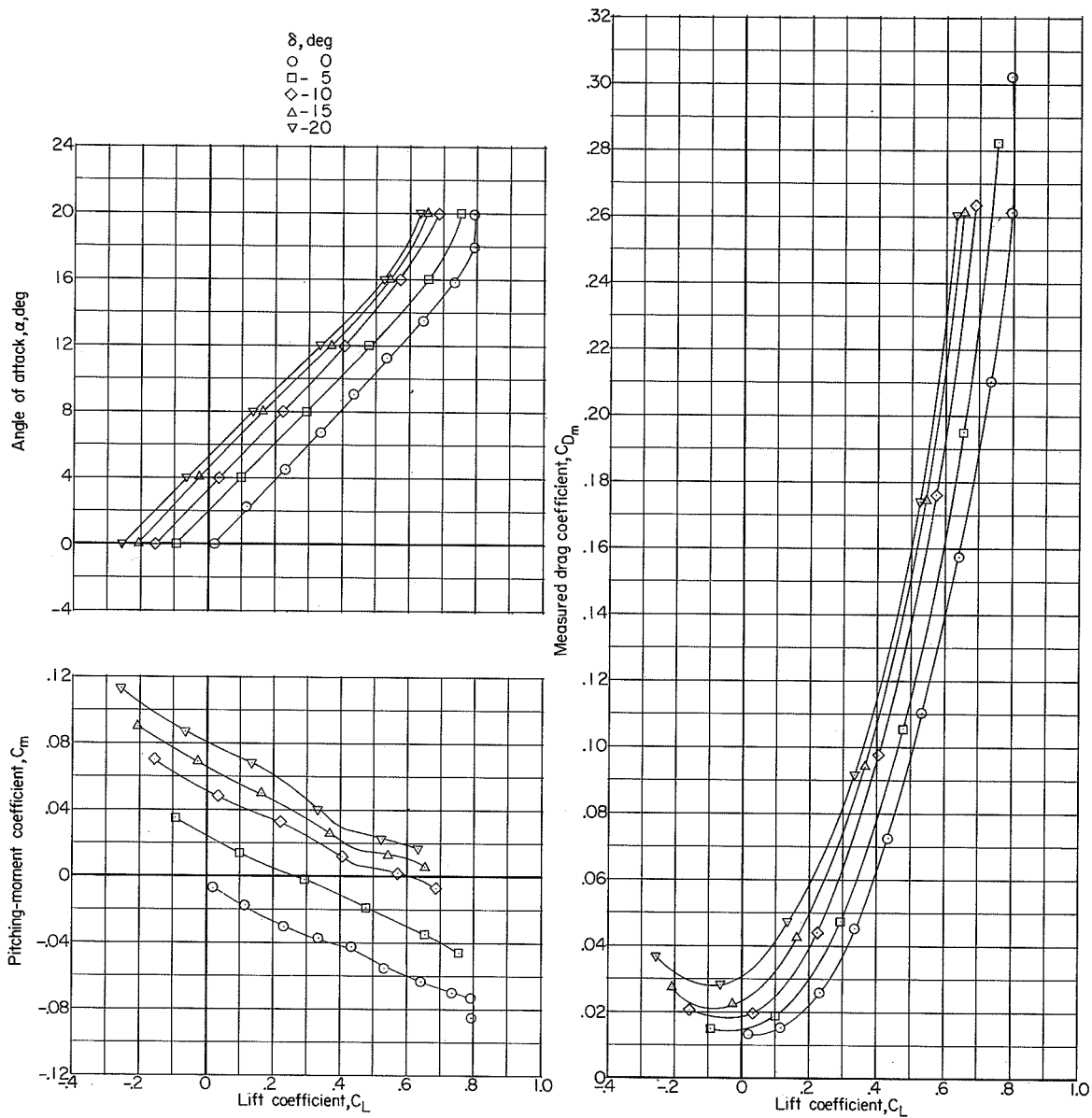
(a) $M = 0.600$.

Figure 5.- Force and moment characteristics of the model with various elevator deflections.



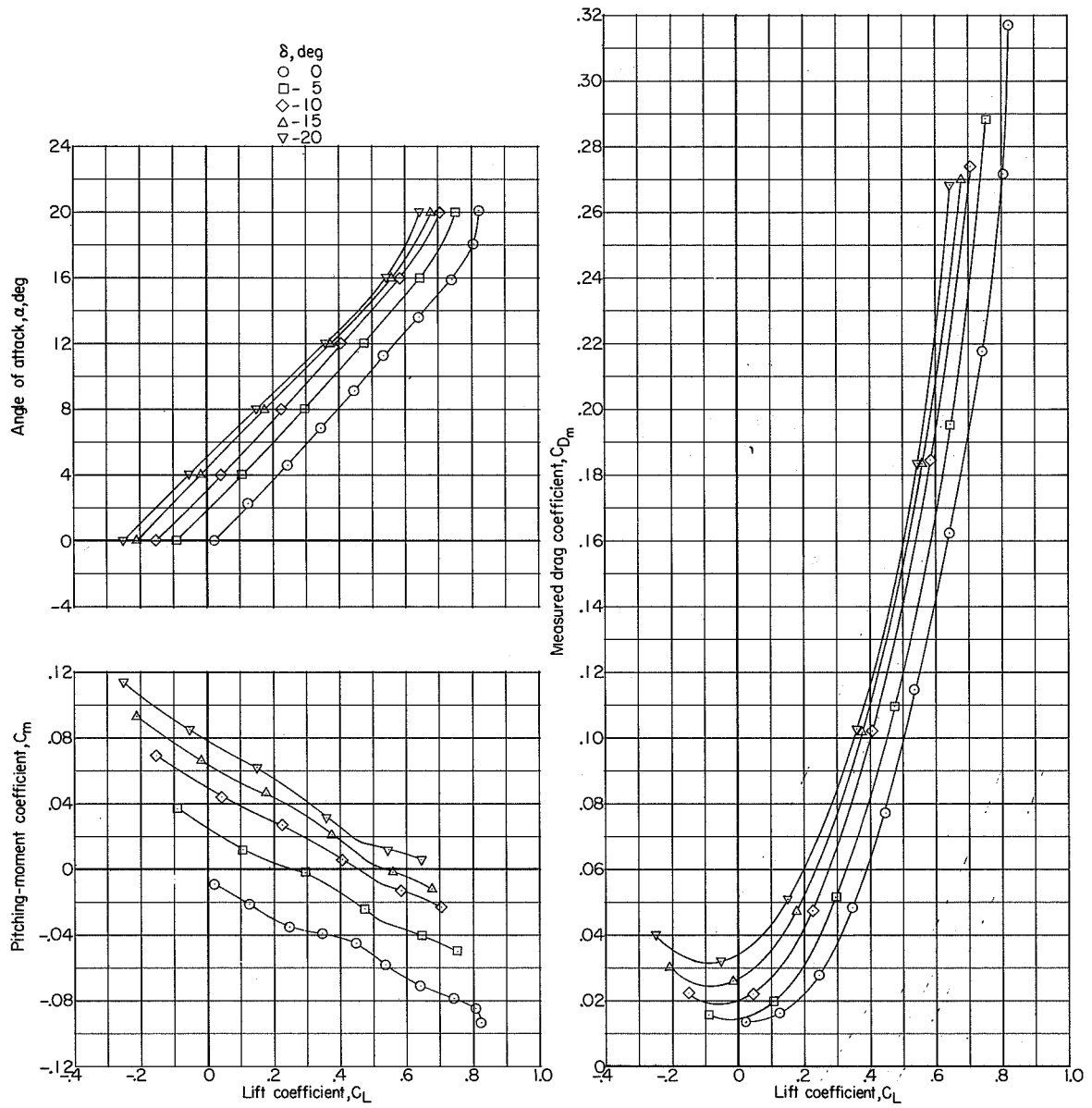
(b) $M = 0.800$.

Figure 5.- Continued.



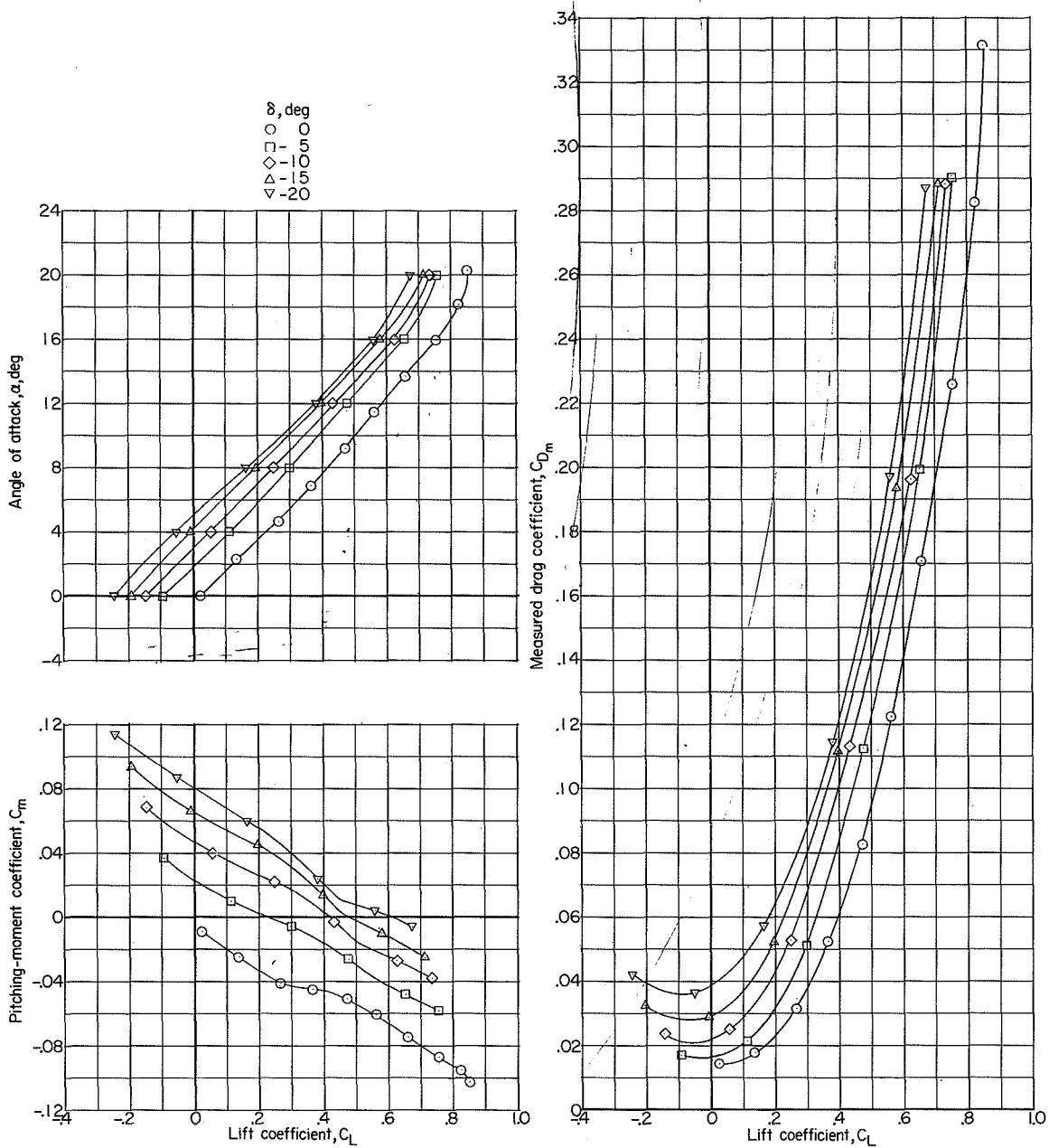
(c) $M = 0.850$.

Figure 5.- Continued.



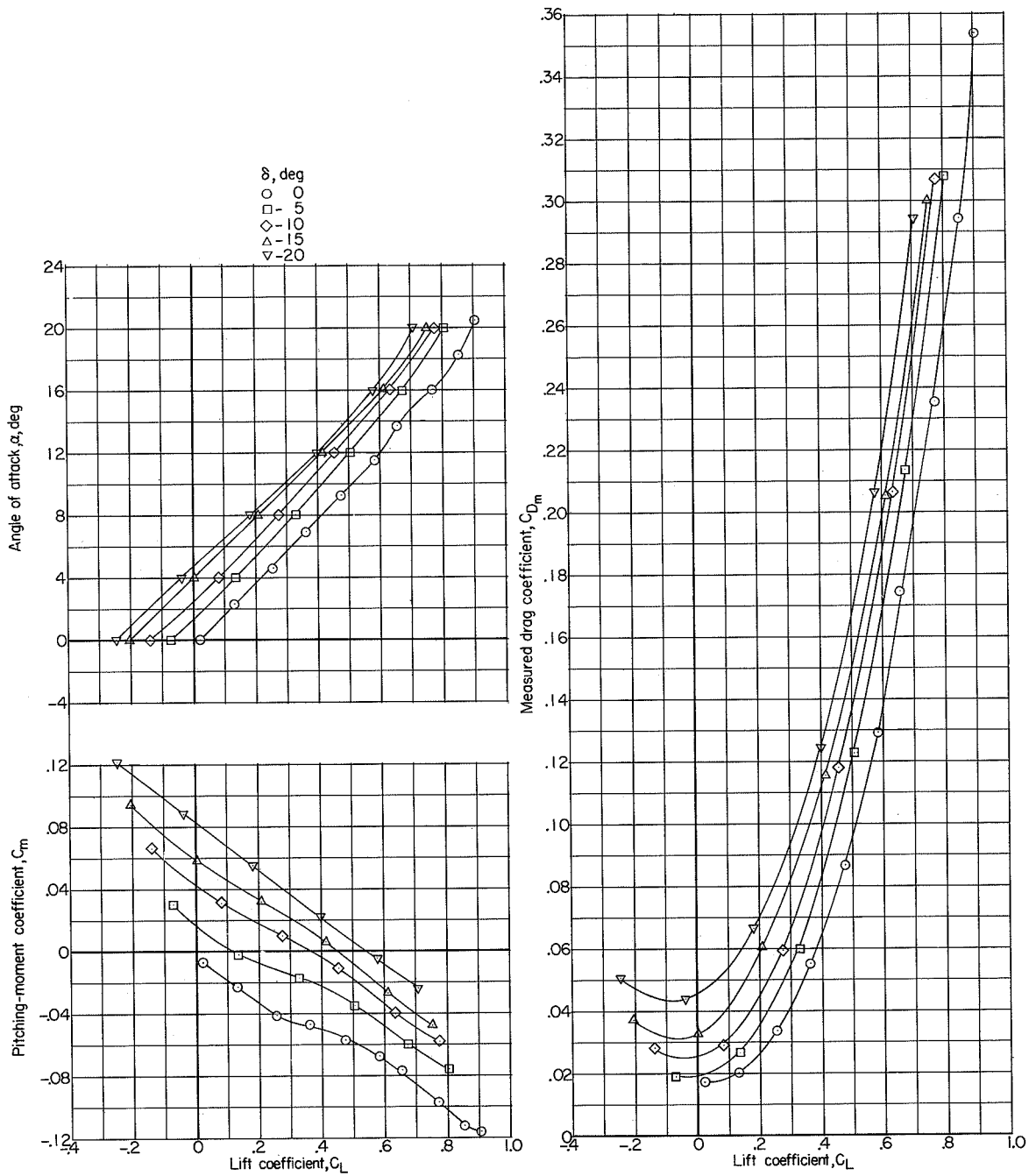
(d) $M = 0.900$.

Figure 5.- Continued.



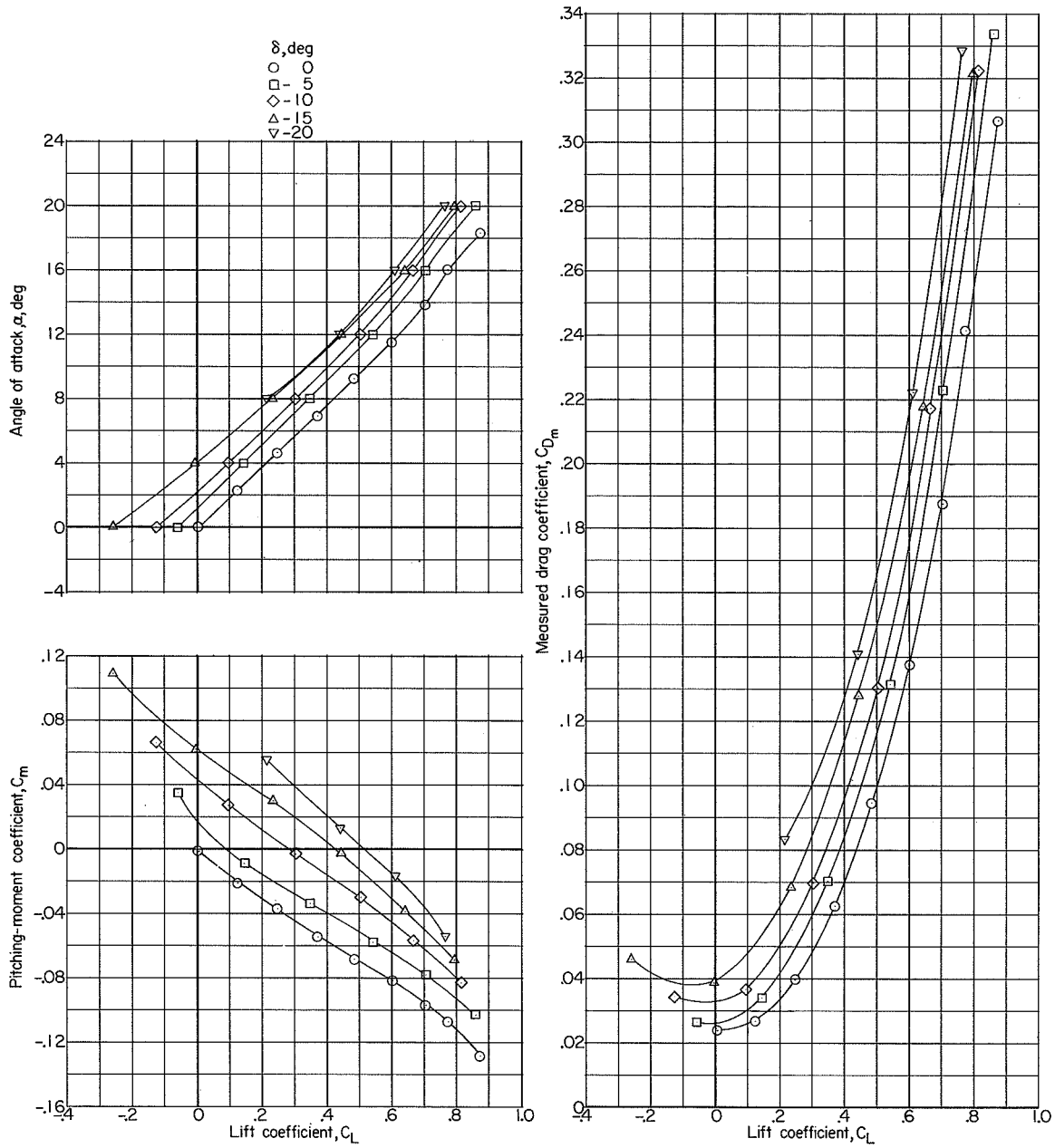
(e) $M = 0.925$.

Figure 5.- Continued.



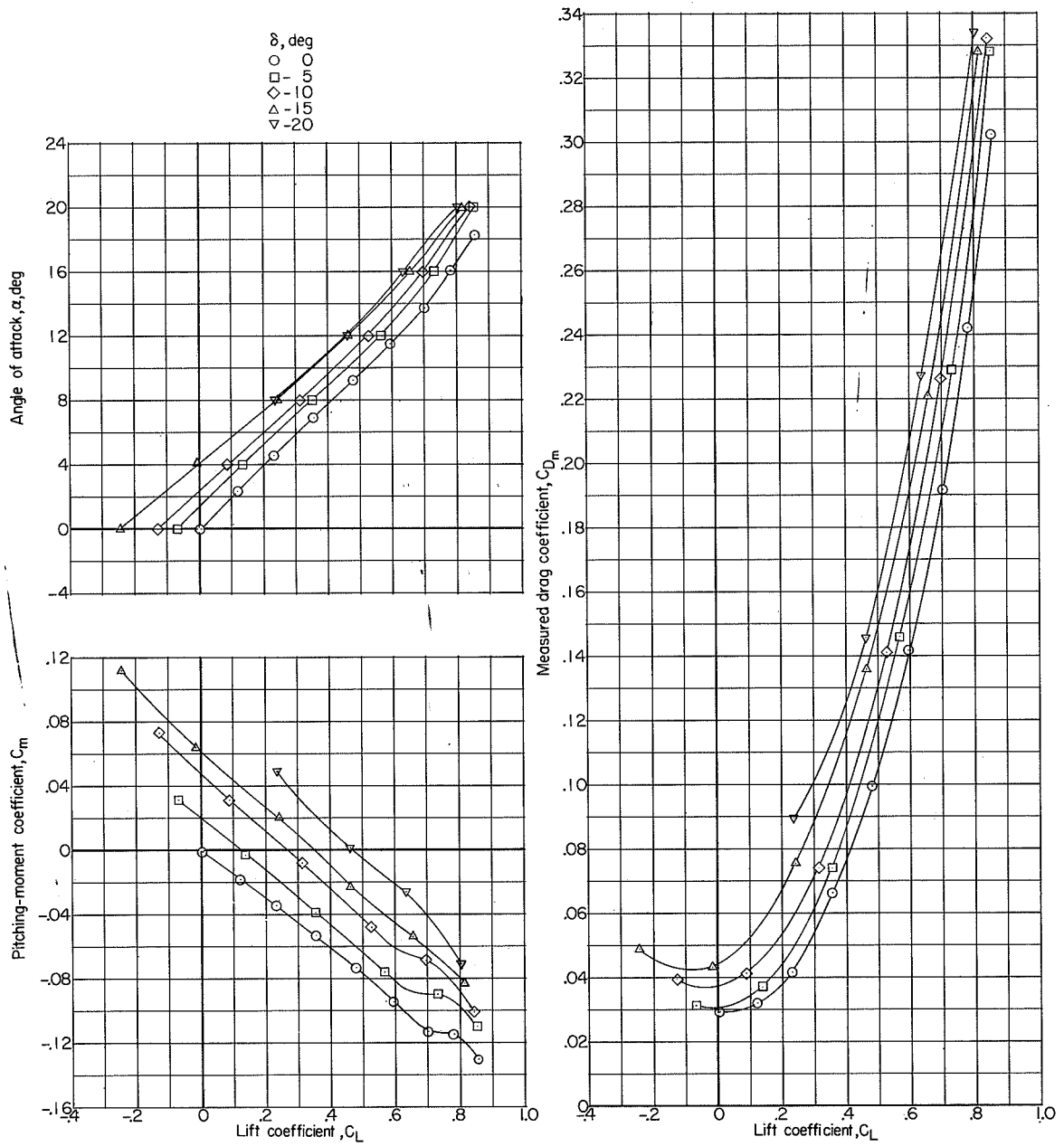
(f) $M = 0.950$.

Figure 5.- Continued.



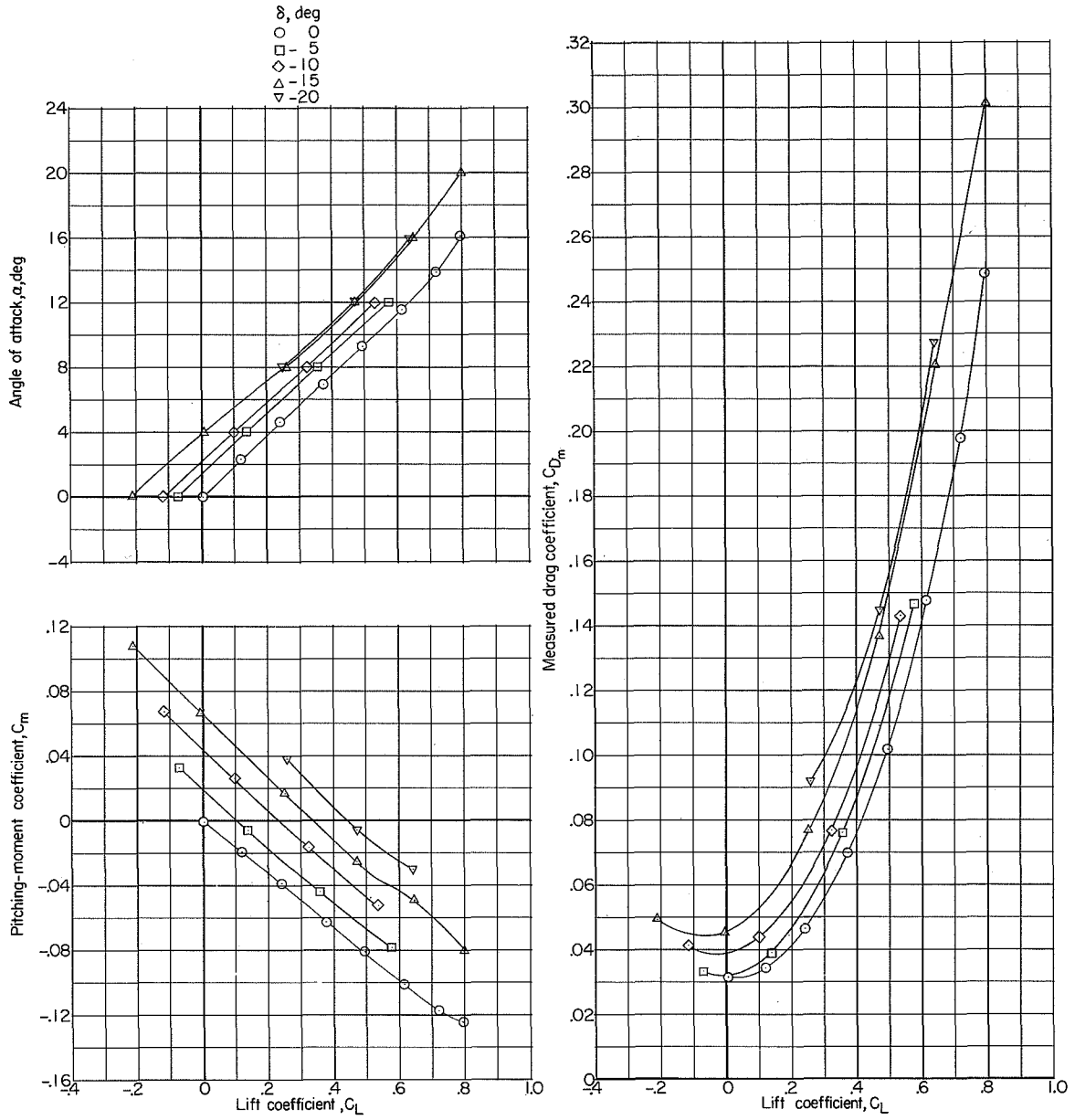
(g) $M = 0.975$.

Figure 5.- Continued.



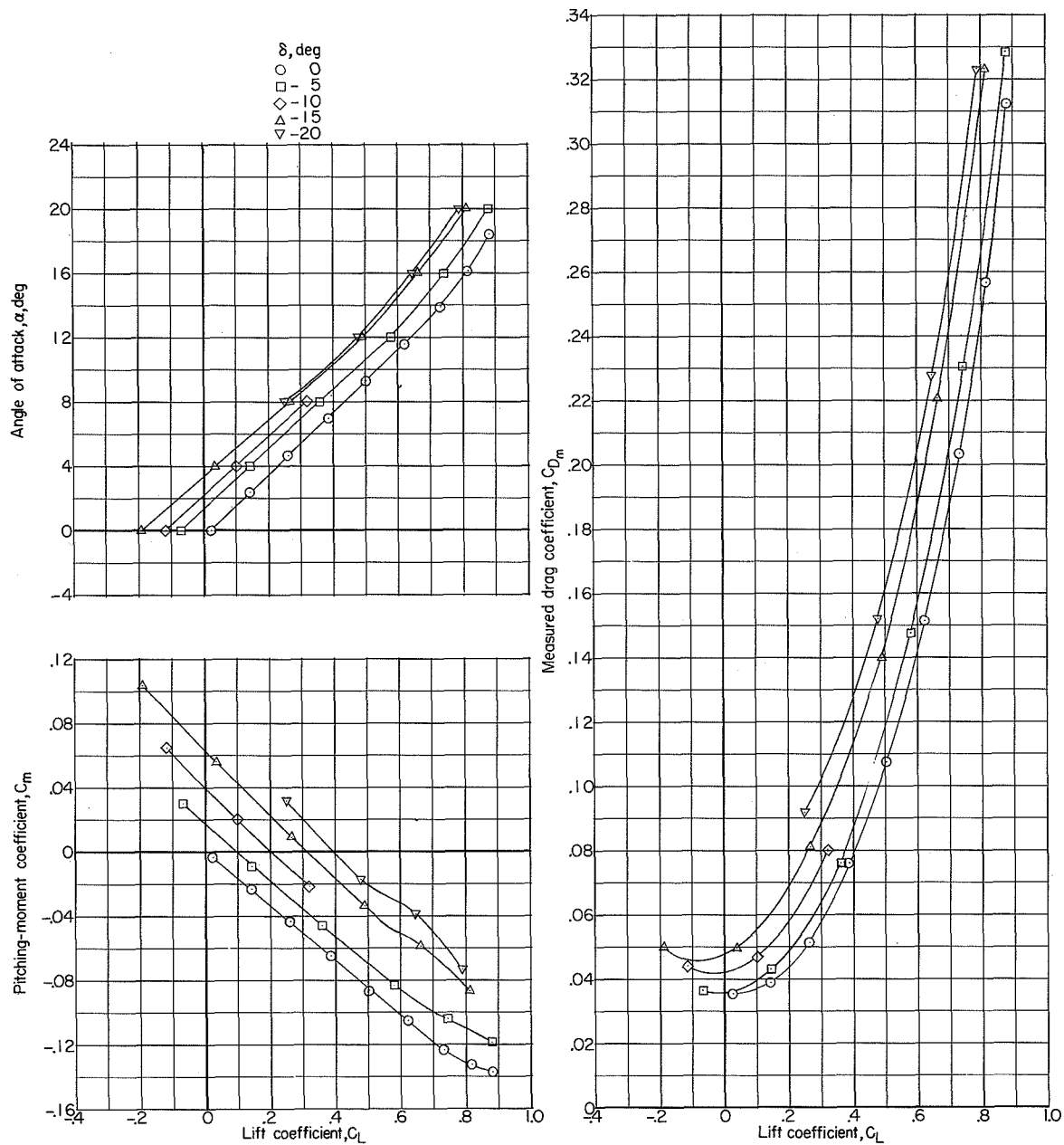
(h) $M = 1.000$.

Figure 5.- Continued.



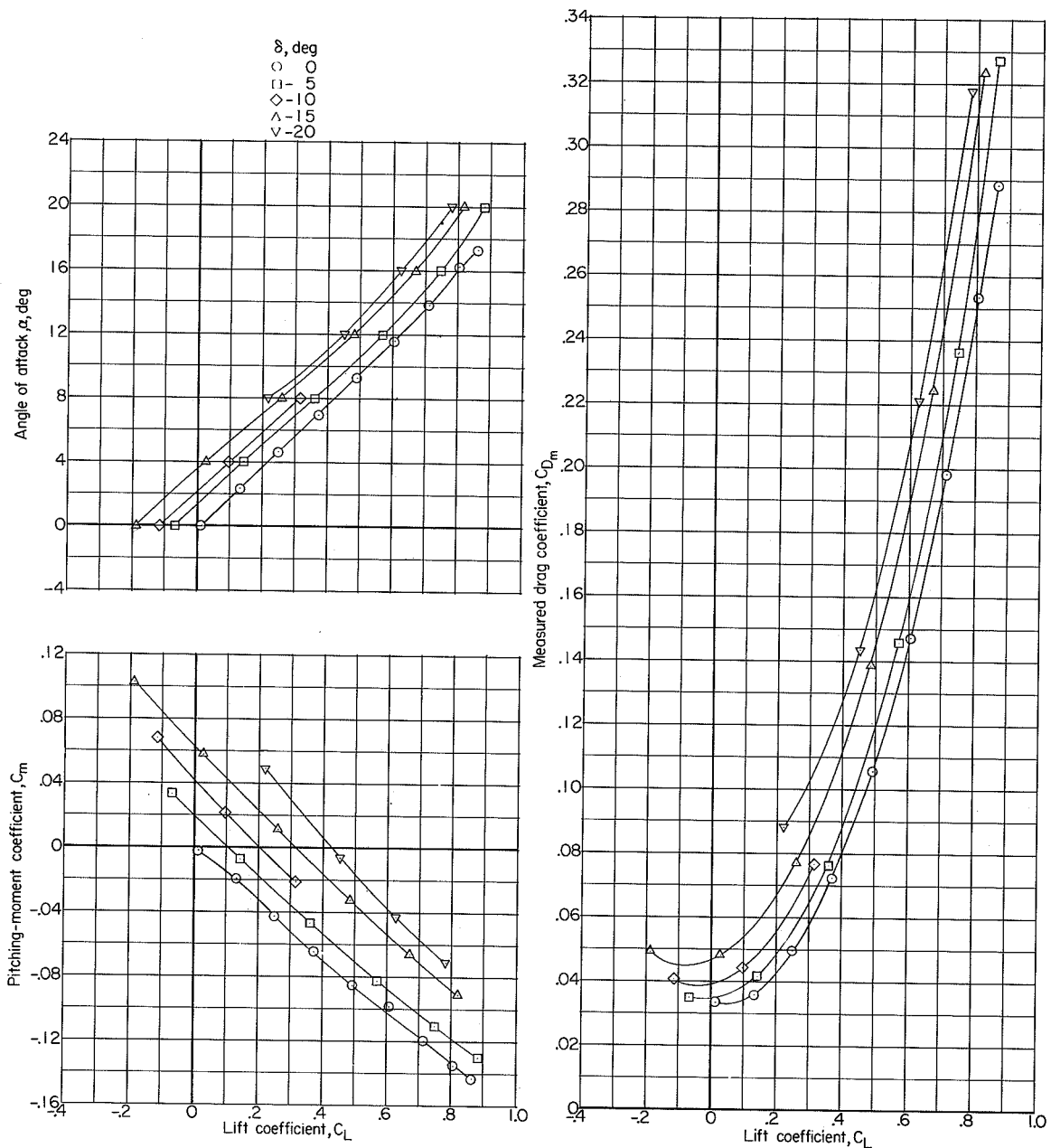
(i) $M = 1.025$.

Figure 5.- Continued.



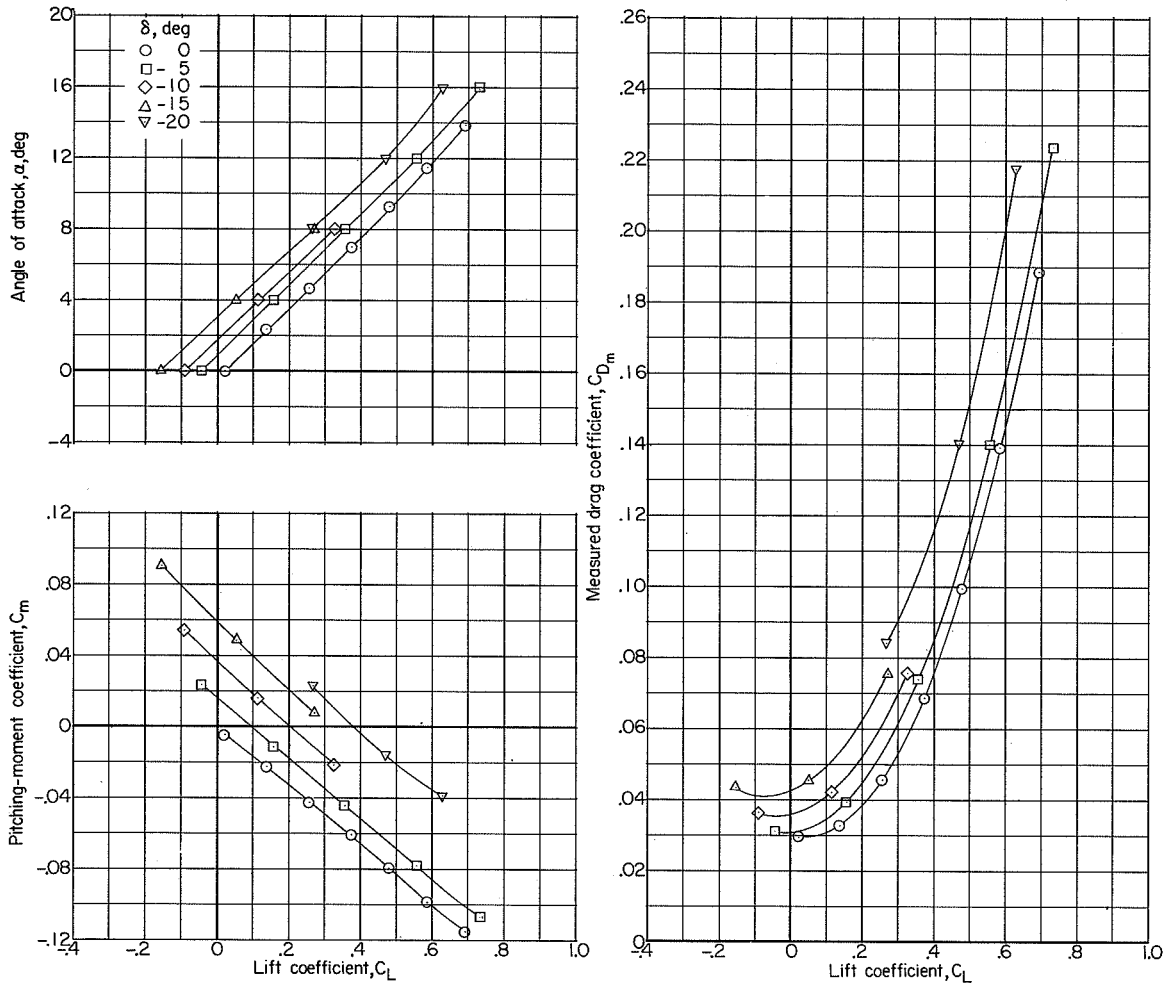
(j) $M = 1.050$.

Figure 5.- Continued.



(k) $M = 1.075$.

Figure 5.- Continued.



(2) $M = 1.100$.

Figure 5.- Concluded.

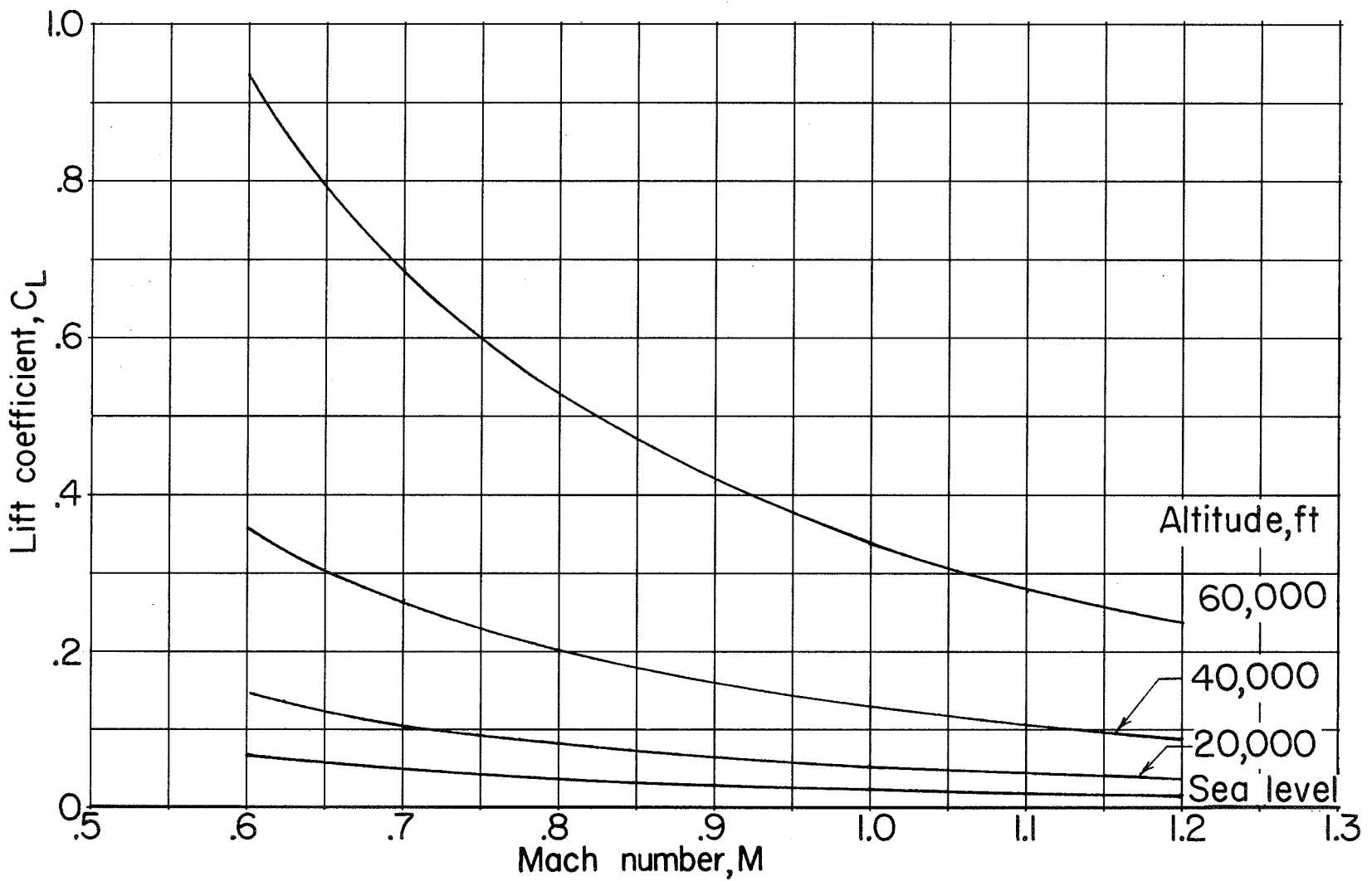


Figure 6.- Variation with Mach number of the lift coefficient required for level flight at several altitudes for a wing loading of 35.4 lb/sq ft.

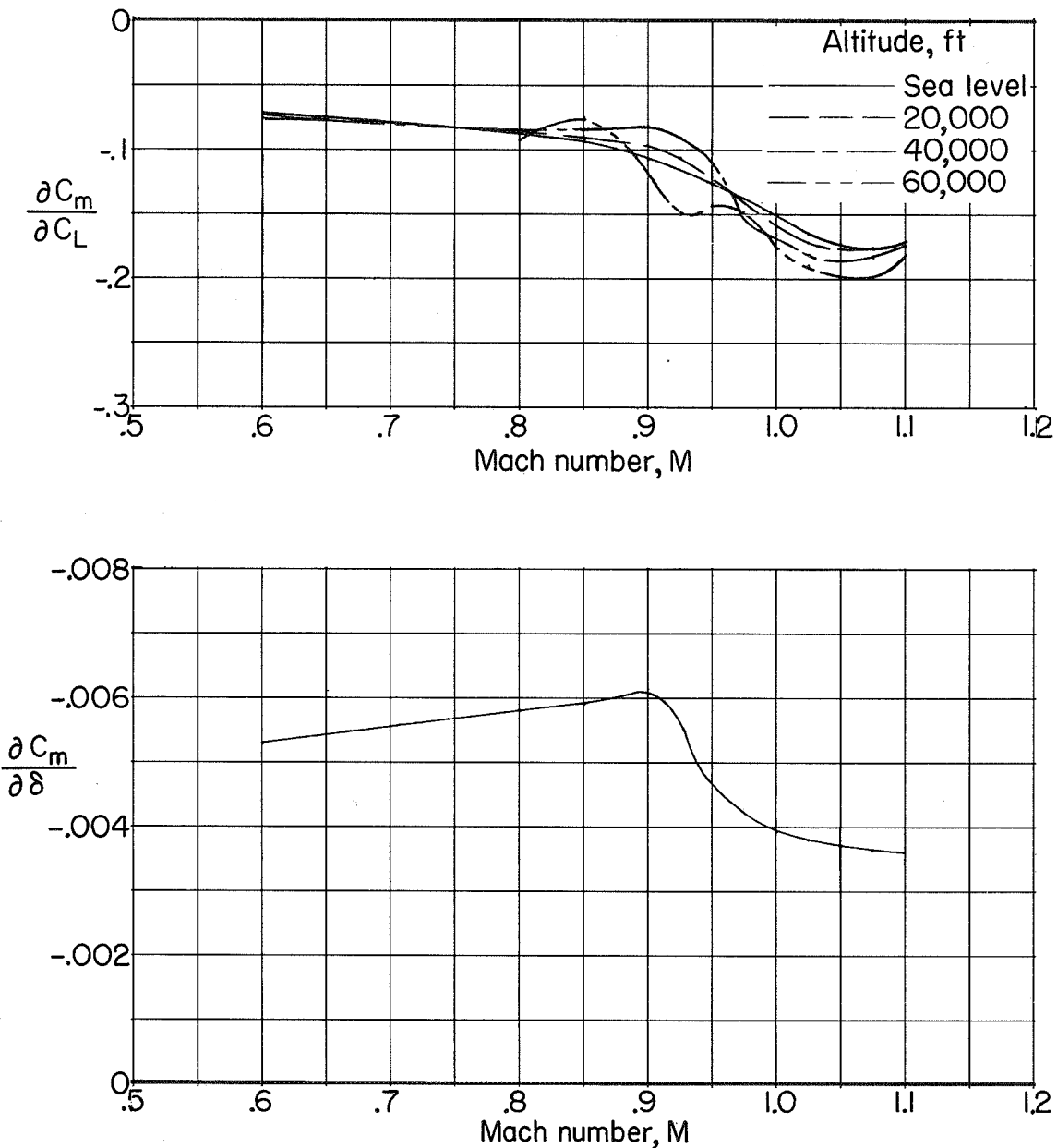


Figure 7.- Variation with Mach number of the trimmed static longitudinal stability parameter and the elevator pitch effectiveness parameter.

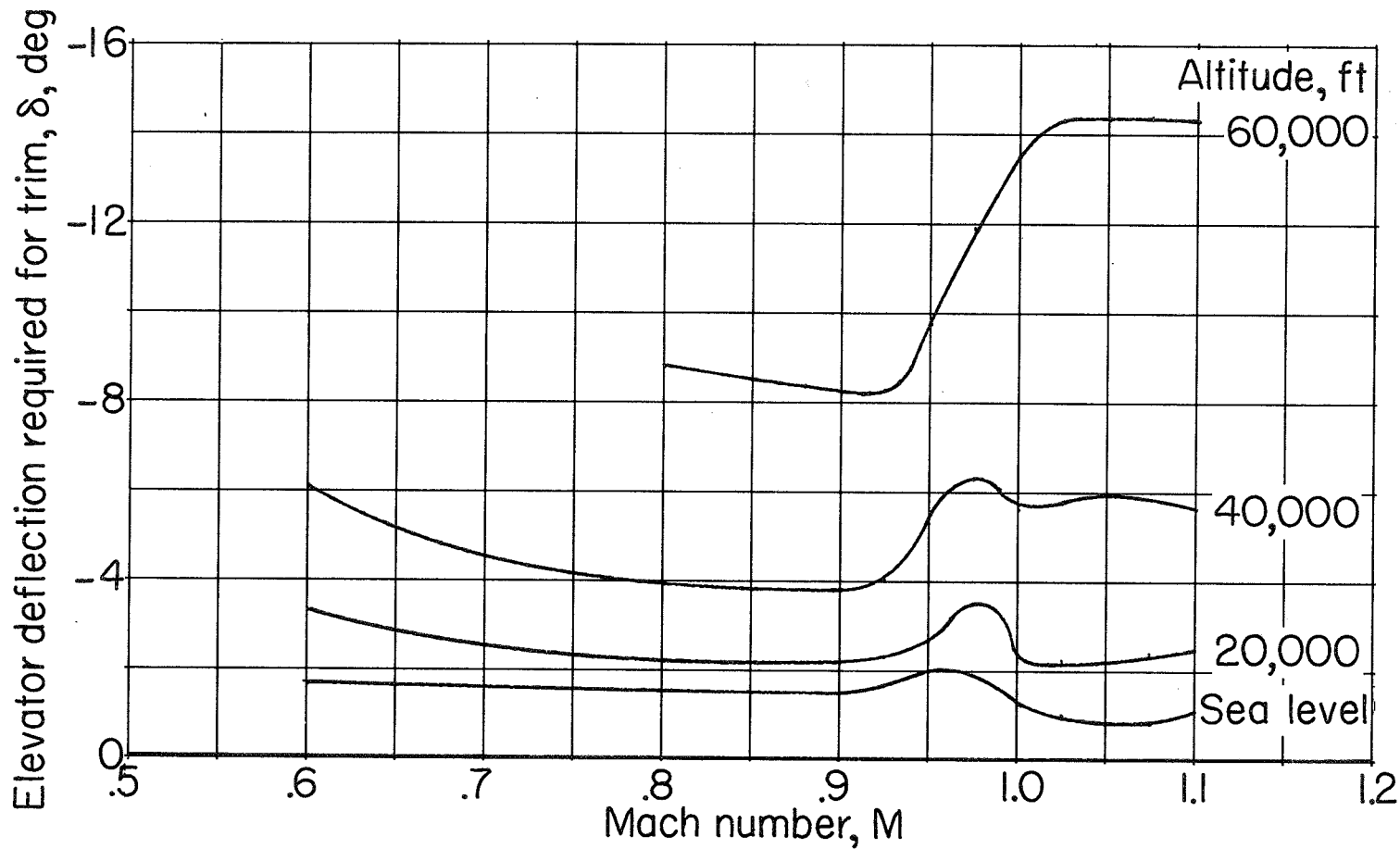


Figure 8.- Variation with Mach number of elevator deflection required for trimmed level flight at several altitudes for a wing loading of 35.4 lb/sq ft.

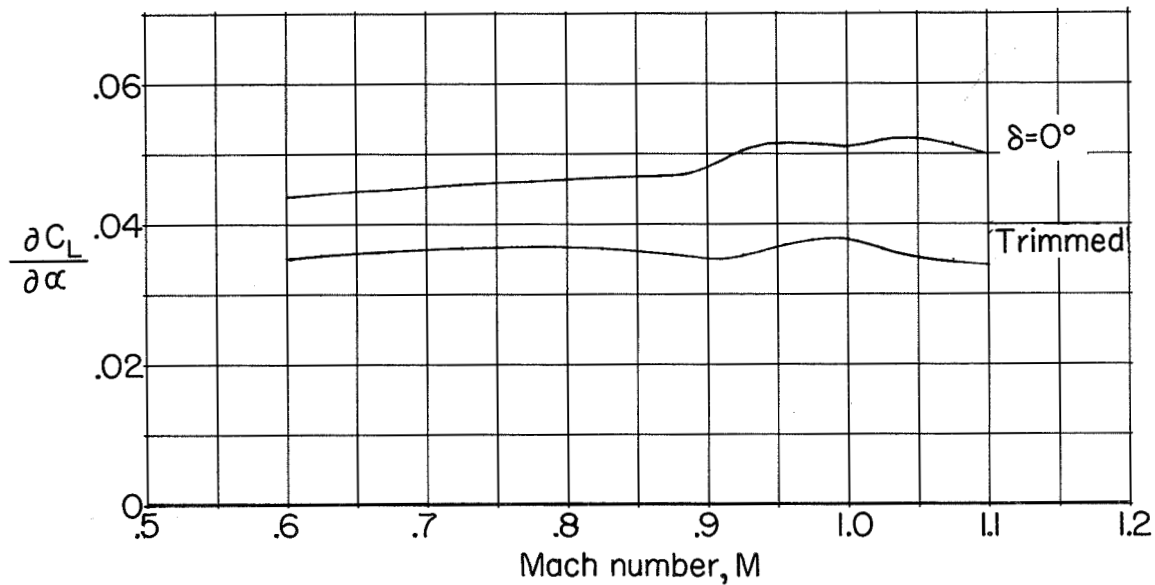


Figure 9.- Variation with Mach number of the lift-curve slope and the elevator lift effectiveness parameter.

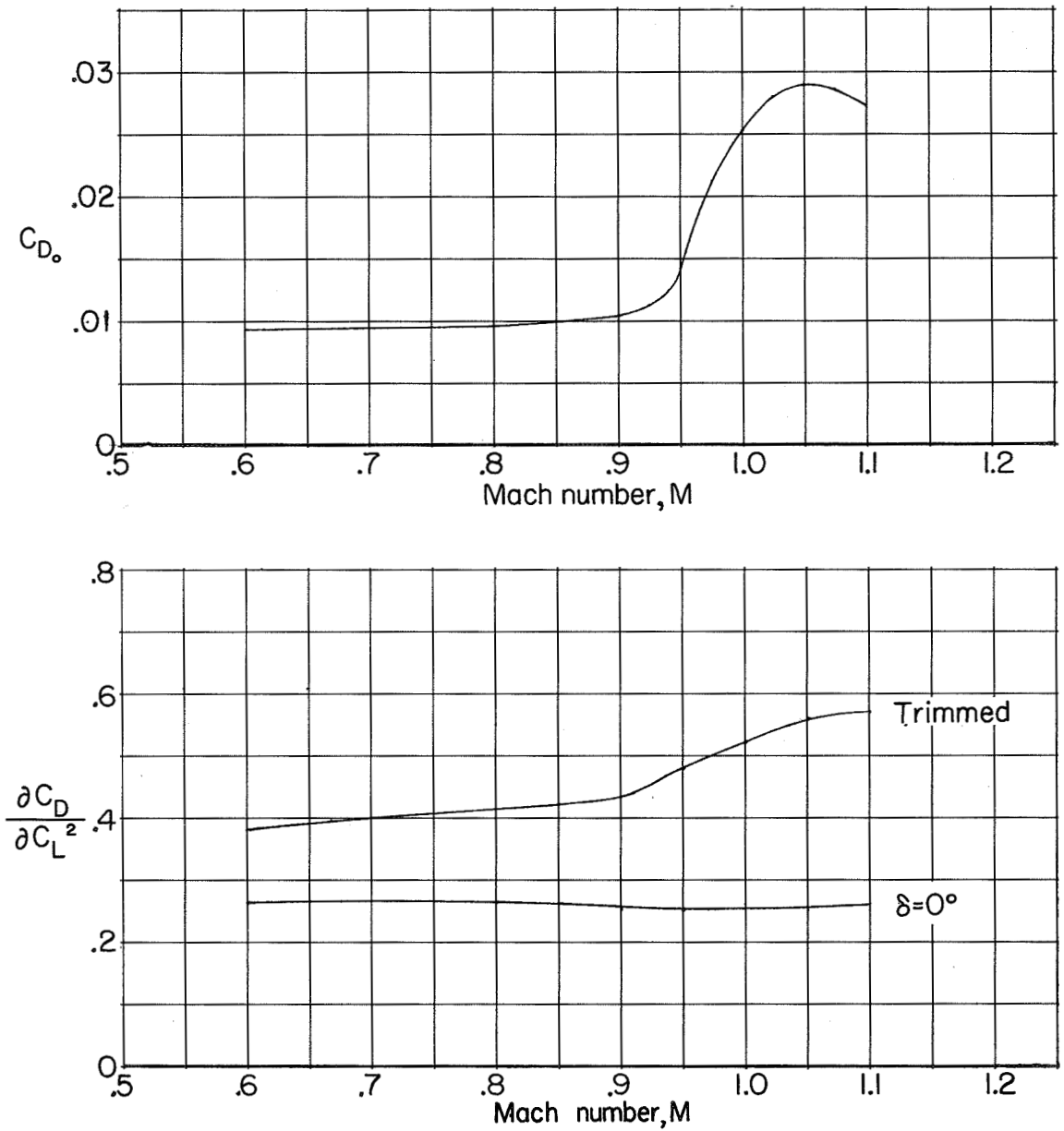


Figure 10.- Variation with Mach number of the drag coefficient at zero lift and the drag-due-to-lift factor. Internal drag removed.

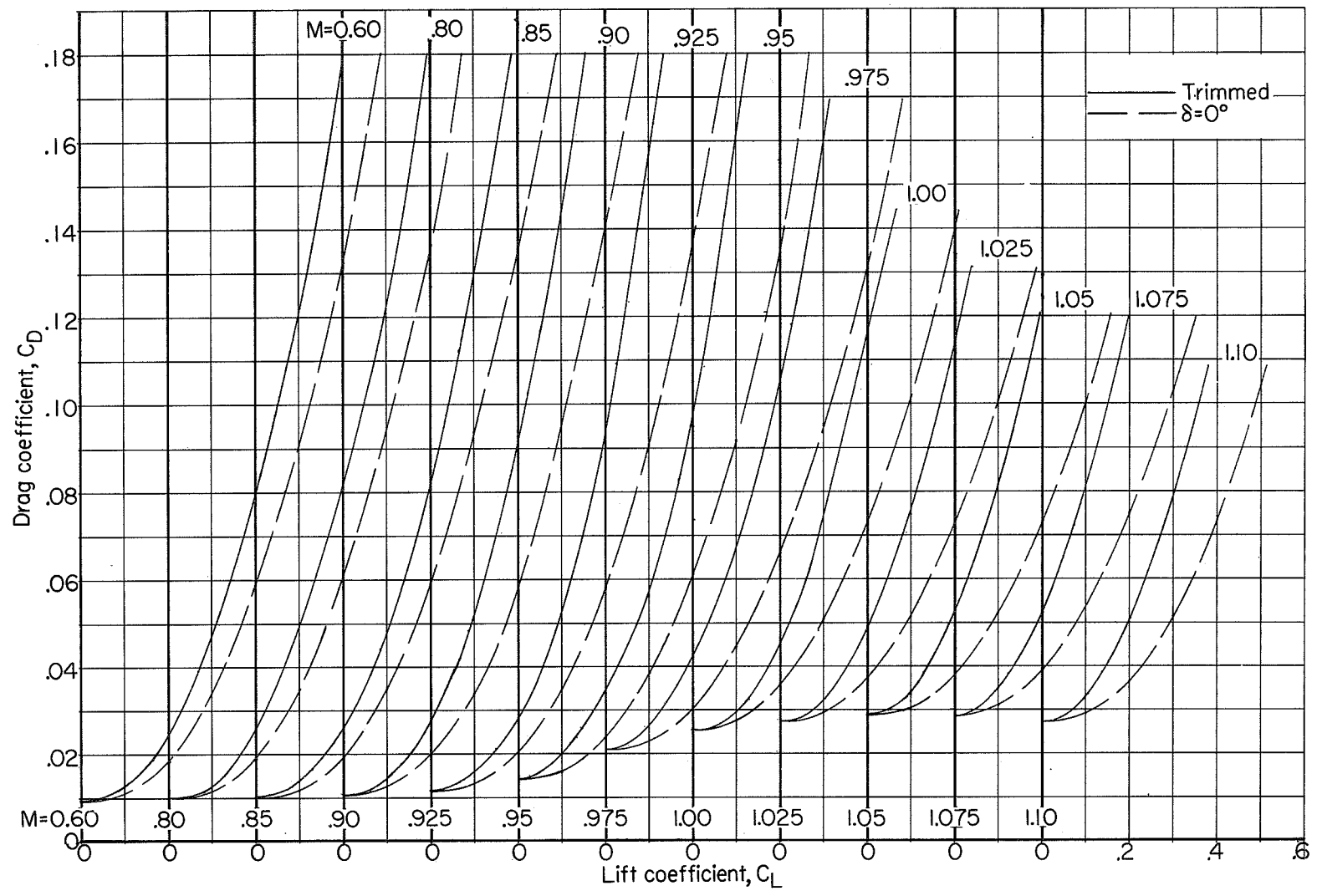


Figure 11.- Variation of drag coefficient with lift coefficient. Internal drag removed.

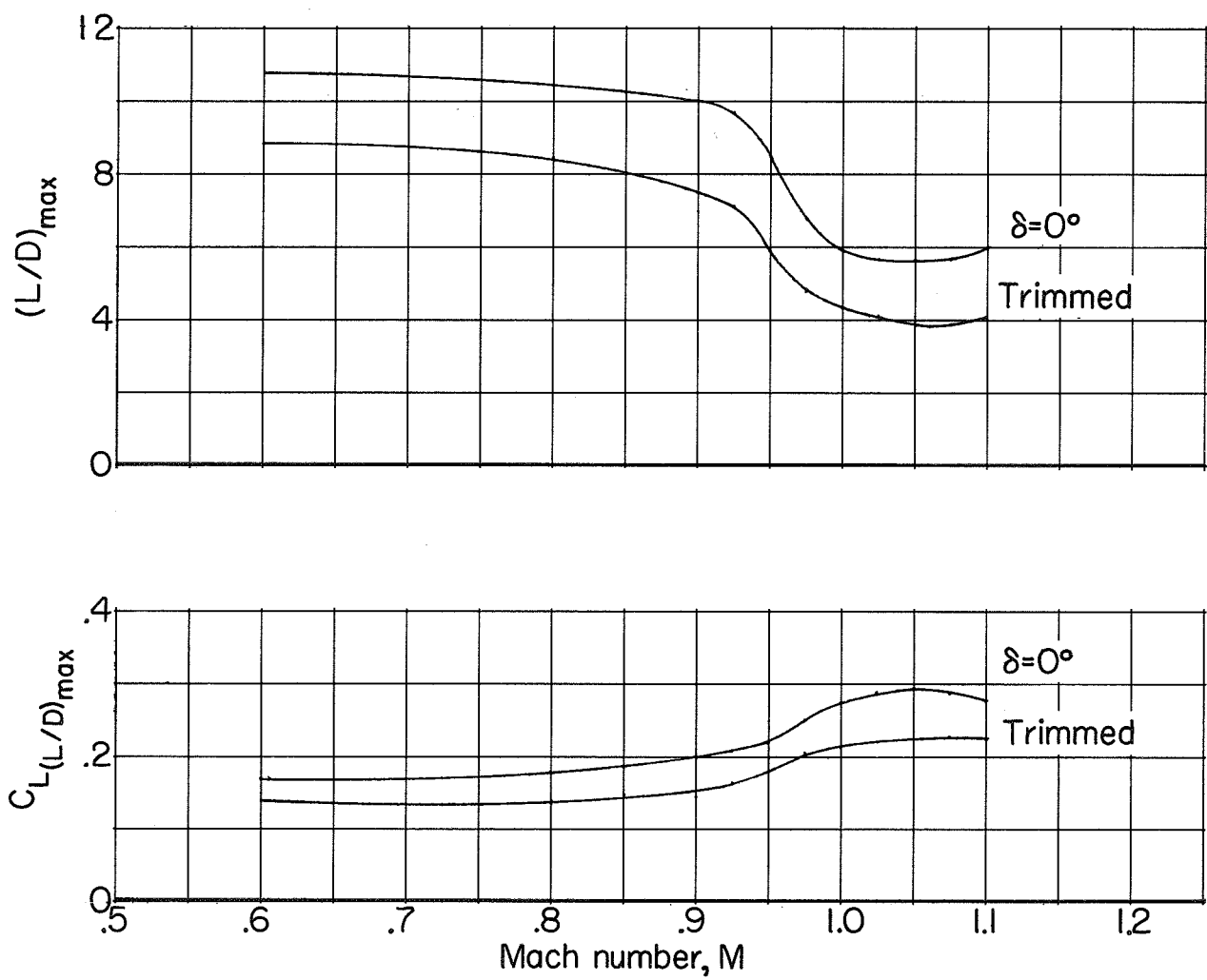


Figure 12.- Variation with Mach number of the maximum lift-drag ratio and lift coefficient for maximum lift-drag ratio. Internal drag removed.

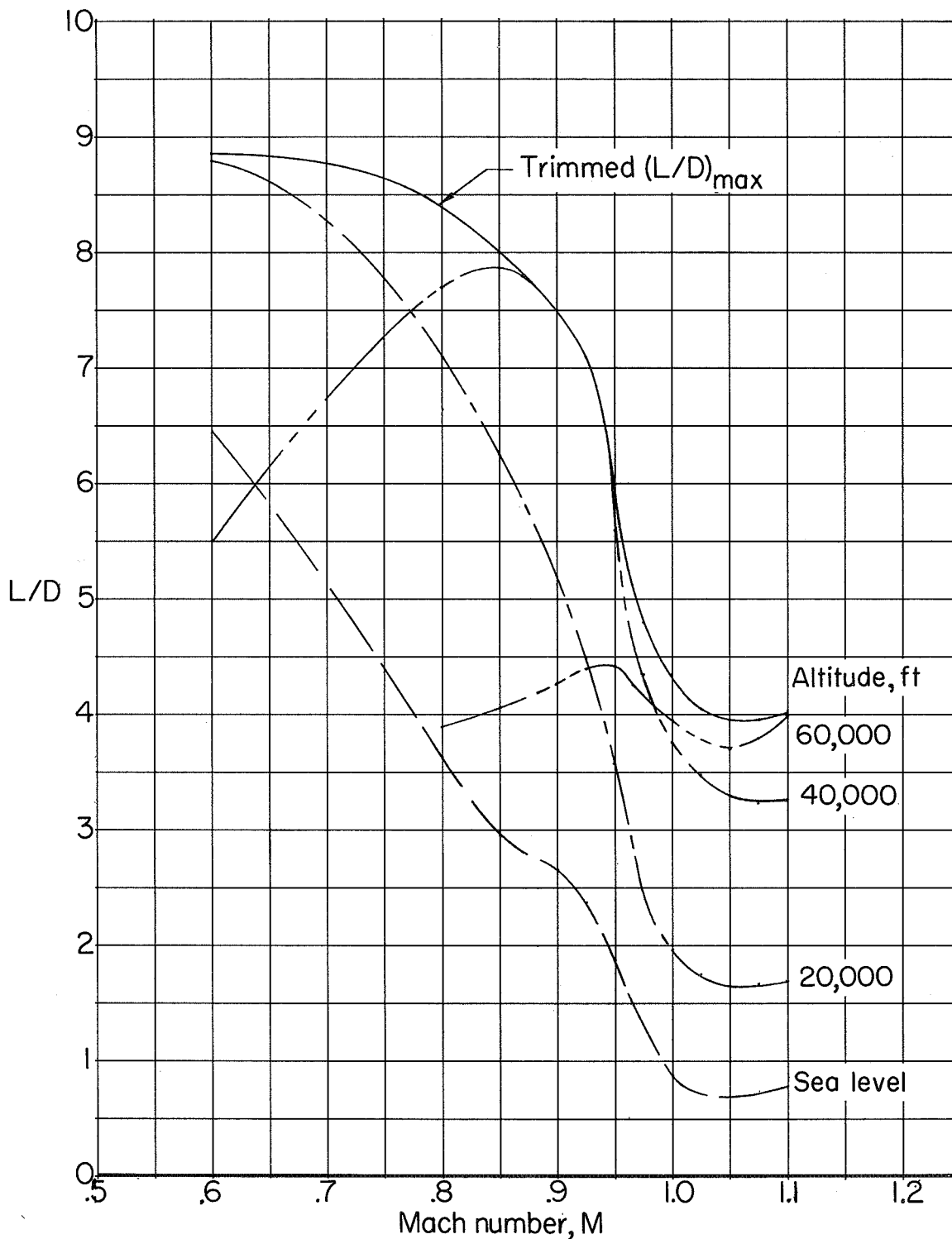


Figure 13.- Variation with Mach number of the maximum trimmed lift-drag ratio and of the trimmed lift-drag ratio in level flight at several altitudes for a wing loading of 35.4 lb/sq ft. Internal drag removed.

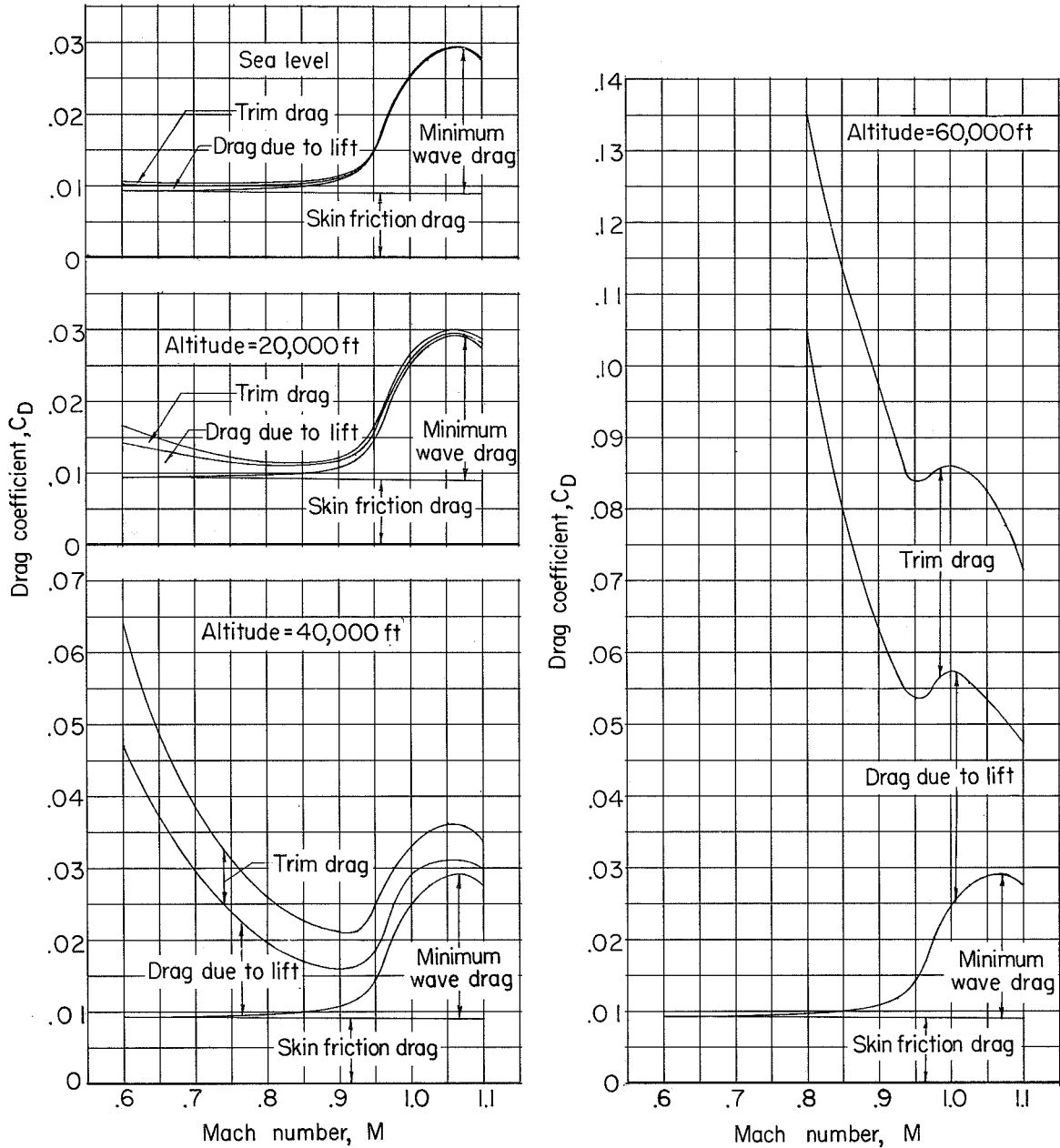


Figure 14.- Drag-coefficient breakdown for trimmed level flight at several altitudes for a wing loading of 35.4 lb/sq ft. Internal drag removed.

Restriction/Classification Cancelled

~~CONFIDENTIAL~~

SECRET

Restriction/Classification Cancelled

~~CONFIDENTIAL~~